FINAL SCIENTIFIC/TECHNICAL REPORT

National Energy Technology Laboratory

THE U.S. DEPARTMENT OF ENERGY

Under Award NO. DE-FE0005865

LARGE SCALE SIMULATIONS OF THE MECHANCIAL PROPERTIES OF LAYERED TRANSITION METAL TERNARY COMPOUNDS FOR FOSSIL ENERGY POWER SYSTEM APPLICATIONS

For the Period: January 1, 2011 to December 31, 2014

PRINCIPAL INVESTIGATOR

Professor Wai-Yim Ching
University of Missouri-Kansas City
Kansas City, Missouri 64110

March 31, 2015

DISCLAIMER*

ABSTRACT

In this final scientific/technical report covering the four year period from January 1, 2011 to December 31, 2014 under NETL support. We report the accomplishments on the study of a unique class of intermetallic compounds, the MAX phases. The main thrust is in the establishment of a large data base of 665 vetted MAX phases and comprehensive evaluation of elastic and mechanical properties, the electronic structure and bonding, and the correlations among them, including creative presentation of the data in graphical form. These studies were based on the new or improved computational methods, collaborations with other research groups, training of graduate students and postdoctoral fellows.

TABLE OF CONTENT

I. EXECUTIVE SUMMARY

Advanced materials with applications in extreme conditions such as high temperature, high pressure, and corrosive environments play a critical role in the development of new technologies to significantly improve the performance of different types of power plants. Materials that are currently employed in fossil energy conversion systems are typically the Ni-based alloys and stainless steels that have already reached their ultimate performance limits. Incremental improvements are unlikely to meet the more stringent requirements aimed at increased efficiency and reduce risks while addressing environmental concerns and keeping costs low. Computational studies can lead the way in the search for novel materials or for significant improvements in existing materials that can meet such requirements. Detailed computational studies with sufficient predictive power can provide an atomistic level understanding of the key characteristics that lead to desirable properties.

This project focuses on the comprehensive study of a new class of materials called MAX phases, or $M_{n+1}AX_n$ (M = a transition metal, A = Al or other group III, IV, and V elements, X = C or N). The MAX phases are layered transition metal carbides or nitrides with a rare combination of metallic and ceramic properties. Due to their unique structural arrangements and special types of bonding, these thermodynamically stable alloys possess some of the most outstanding properties. We used a genomic approach in screening a large number of potential MAX phases and established a database for 665 viable MAX compounds on the structure, mechanical and electronic properties and investigated the correlations between them. This database if then used as a tool for materials informatics for further exploration of this class of intermetallic compounds.

II. PROJECT DESCRIPTION

In the original statement of project objectives (SOPO) at the beginning of the project, The following objectives were listed: (1) to understand the fundamental mechanical and electronic structures of the MAX phase alloys and to predict the useful new phases; (2) to perform multi-axial compression and tensile experiments on selective MAX alloys on DOE supercomputers in order to have a better description of their deformation behavior; (3) to develop new methods for calculating thermomechanical properties at elevated temperature and pressure starting form *ab initio* calculation of the phonon spectra; (4) to explore the effects of grain boundaries and interfaces of the MAX phase materials with and without segregated ions via large scale structural modeling including spectroscopic characterizations; and (5) to establish collaborations with experimental scientists at DOE laboratories and other academic institutions to accelerate the materials development for fossil energy technology.

The scope of the project is rather extensive involving following 7 tasks which are finely divided into subtasks (except task 1 and 7). It includes the calculation of the electronic structure and mechanical properties of a limited number of MAX phase alloys judged to be special or important at that time. The scope of the work is roughly divided into two phases. Phase I (first 2 years) will cover the areas of fundamental mechanical properties, electronic structure and bonding of MAX phase alloys, and execution of the multi-axial tensile/compression simulations. Phase II (third

year) focuses on mechanical properties at high temperature, pressure, and corrosive environments together with modeling and simulation studies of microstructures and interfaces in MAX phase materials. These 7 tasks are succinctly listed as follows:

Task 1 Project Management and Planning

Task 2 Fundamental mechanical properties of MAX phases

These include the following MAX phase alloys: Ti_3AlC_2, Ti_2AlC, Ti_3SiC_2, Ti_2AlN, Cr_2AlC, Nb_2AsC, Nb_4AlC_3, Zr_3AlN, $Zr_3Al_3C_5$, $Zr_2Al_3C_5$, Hf_3AlN, $HfAl_4C_4$.
Subtask 2.1: Calculation of the elastic constants and mechanical properties of five crystals: Ti3AlC, Ti2AlC, Ti3SiC2, Ti2AlN, and Cr2AlC.
Subtask 2.2: Lattice phonon calculations of the same five crystals as above.
Subtask 2.3: Extension of the above calculations to the other phases alloys.

Task 3 Electronic structure and spectroscopic properties of MAX phases

Subtask 3.1: Calculation of the electronic structure, interatomic bonding and charge distributions of the same MAX phases as in subtask 2.1.
Subtask 3.2: Calculation of the interatomic bonding and effective charges for the same MAX phases.
Subtask 3.3: Connection between mechanical properties and electronic structure for MAX phase alloys.

Task 4 Multi-axial tensile and compression simulations on some MAX phases.

Subtask 4.1: Multi-axial simulations on Ti3AlC2, Ti2AlC, Ti3SiC2, Ti2AlN, and Cr2AlC.
Subtask 4.2: Multi-axial simulations will be extended to a few other alloys.
Subtask 4.3: Construction of 3-D failure envelope in both strain and stress spaces for MAX phases.

Task 5 Mechanical properties at high temperature and pressure

Subtask 5.1: Based on results of Tasks 1 and 3, a few selected alloys will be targeted for temperature and pressure dependent mechanical prosperities. Extensive testing of codes and improvements for efficiency.
Subtask 5.2: Following subtask 5.1, similar investigation on a few promising composite models.
Subtask 5.3: As part of task 7, implementation of improved codes on different computer platforms.

Task 6 Modeling of microstructures and interfaces and the effect of corrosion using supercells

Subtask 6.1: Model grain boundary structures in selective MAX alloys and investigate their mechanical properties. Calculation of core level spectra for atoms in models as part of structural characterization.

Subtask 6.2: Model interface structures between the MAX phases and oxides, investigate their mechanical properties and structural characterization using XANES/ELNES spectral calculations.
Subtask 6.3: Model ions segregated to grain boundaries and interfaces to investigate corrosive effects.

Task 7 Development of computational algorithms and codes

The majority of above tasks have been completed. However, near the end of the second year, it becomes apparent that rapid development of research on MAX phases in relation to their possible applications and stiff competition from better funded international teams rendered it necessary and urgent for expansion in the MAX phases covered and a refocus on the properties to be investigated. A shift in strategy and focus of project goals in order to increase the impact of the research on this NETL supported project is imperative. With the approval of the Technical Monitor, we proposed a modification and expansion in tasks together with a request of a one-year no-cost extension of the project. Significant results were obtained mostly in the last two years of the four year period. These accomplishments are described in section III.2.

III. REPORT DETAILS

III.1 Computational Methods

In this computational project, we used two well recognized quantum mechanical methods for extensive simulations: (1) The Vienna *Ab initio* Simulation Package (VASP), and (2) the first-principles orthogonalized linear combination of atomic orbitals (OLCAO) method. VASP is an *ab initio* code based on density functional theory (DFT) using plane-wave basis expansion and pseudopotentials and is fully parallelized on supercomputers. It is one of the most popular electronic structure codes especially for geometry optimization, accurate force calculation and evaluation of elastic and mechanical properties. More recently, for extensive modeling on composite alloys and for a few selected MAX phases, we have also used for the newly implemented version of VASP with *ab initio* molecular dynamics (AIMD). This enables us to study the temperature dependent properties.

The OLCAO method is another DFT-based *ab initio* computational package developed in our own laboratory over the last thirty years. It is extremely efficient and versatile for electronic structure and bonding calculation of large complex systems due to the flexible choice of the atomic basis set expressed in Gaussian type of orbitals and analytic evaluation of all interaction integrals. It enabled us to couple with the VASP code to use the high throughput genomic approach in calculating a large number of MAX phases. OLCAO method is instrumental in establishing the new concept in using the total bond order density (TBOD) as a single effective quantum mechanical metric is the evaluation materials properties including the MAX phases.

We have also implemented other computational schemes and techniques to speed up on calculations and in analyzing vast amount of data obtained including innovative display of results for easy dissemination and understanding of the MAX phases and their inter-correlations in connection to data mining and machine learning strategy within the theme of materials informatics.

III.2 Results and Discussions

The major accomplishments for the project are succinctly summarized below with the relevant publications numbered and listed in section VI. Bibliography. They are not in the chronological order but are roughly in the descending order of importance and impact.

A. Comprehensive database of all stable MAX phases. (13)

An extensive database for the structural, mechanical and electronic properties of 665 MAX phases has been established and made publicly available. The Editor of the Journal Phys. Status Solidi – B selected this article for the journal cover page. The paper has also introduced the new concept of using TBOD for correlating different properties of MAX phases. This is the main achievement of this project which puts the research on MAX phases in US supported by NETL firmly among the best internationally.

B. Electronic structure and mechanical properties of 20 MAX phases. (2,4,5,7)

This part of the work is the major accomplishment in the study of MAX phases in the early part of the research phase. It went well yond the phases specified in the SOPO and prompted the change in the research direction that resulted in the genomic approach of investigating all potentially stable MAX phases (see A above). This work has attracted a lot of attention in the international community because of the scope of the work involved and the publications have already garnered a large number of citations.

C. Identification of structure and properties of a new MAX derived phase, $(Cr_2Hf)_2Al_3C_3$. (12)

This is an innovative piece of work as part of the Ph.D. dissertation of Dr. Yuxiang Mo under this support. It is one of the original tasks listed in SOBO for other layered MAX like structures. New stable MAX-like phase is predicted to exist which can stimulate laboratory search for this and other new phases. The paper has been selected as a Key Scientific Article contributing to excellence in engineering, scientific and industrial research by Target Selection Team at Advances in Engineering and featured in Advances in Engineering Series.

(http://advanceseng.com/instructions-authors/)

D. XANES/ELNES spectral calculation of 7 MAX phases compounds. (8)

This work is under the original task 6.1 in SOPO. We are the first group to study the core level spectra in 5 MAX phases with results in good agreement with experiments. The calculations cover the Ti-K, Al-K, Cr-K, Nb-K, C-K edges in 5 MAX phases (Ti_2AlC, Ti_2AlN, Ti_3AlC_2, Cr_2AlC and Nb_2AlC). Results on 2 other phases (Ti_2SiC and Ti_3SiC_2) have also been obtained recently but have not published.

E. Surface adsorption of O atom and O_2 molecules on Cr_2AlC (0001) surface. (10,14)

This is part of the original task 6.3 to investigate the corrosion resistance of MAX phases using Cr_2AlC as an example and also involved in the development and use of *ab initio* molecular dynamic code. This work was not completely finished due to the early departure of the postdoctoral

fellow Dr. Neng Li dual to lack of resources at the later part of the project. However, it does demonstrate that the approach we used can be effective for such studies on MAX phases.

F. Study of lattice thermal conductivities at high temperature. (16)

This was not listed as a major task in the original SOPO. However, after the revised focus of the project and with the large database on many MAX phases available (see item (A)), it becomes apparent that we can use the elastic coefficient data to obtain the approximate values of lattice thermal conductivities at high temperature. No such calculations are available in the literature. The calculated data can be used to explore potential high temperature applications of the MAX phases.

G. Calculation of universal elastic anisotropy A^U in all stable MAX phases. (19)

This is one of the last projects conducted under this grant. The work is based on the recent theory by Ranganathan and Ostoja-Starrezewski, (Phys. Rev. Lett., 2008). Using the data from item A for the MAX phases, the A^U for 665 MAX phases have been completed and a manuscript on it is under preparation. Once published, this work will have a significant impact because we find that the majority of MAX phases have low universal elastic anisotropy in stark contrast with conventional thinking in relation to its anisotropic lattice structures.

H. Computational method development and implementation. (1-19)

This is part of the Task 7 in the SOPO which has been conducted throughout the entire funding period. It covers all the work related to computational method and code development, implementation on different platforms, and testing new programs and techniques for creative graphic presentations.

I. Extending to other MAX related systems: solid solution and Mxenes. (15,18)

This part of research can further expand the scope of applications of MAX phases, or from ternary alloys to quaternary alloys. The only published work is on the $Ti_2Al(C_xN_{1-x})$ solid solution using the supercell approach. There are far more MAX solid solutions than the MAX phases which can potentially increase the synthesis and applications of MAX related compounds.

J. Innovative graphic presentation of massive data obtained. (13, 19)

This includes the presentations in the form of MAPs mimicking Periodic Table and some of the figures shown in Section IV.

K. Other accomplishments

(1) Support and training of graduate students with degrees completed.

Yuxiang Mo, MS, (2011).
Chandra Dhakal, MS (2015)
Liaoyuan Wang, Ph.D (2013).
Yuxiang Mo, Ph.D (2014)

(2) Training and support of postdoctoral researchers and senior researchers.

Dr. Neng Li,
Dr. Sitaram Aryal
Dr. Altaff Hussain

Dr. Ridwan Sakidja

(3) Establishment of external collaborations

Professor Michel Barsoum, Drexel University
Professor Lizhi Ouyang, Tennessee State University
Professor Jiangyang Wang, Institute of Metals, Chinese Academy of Sciences

III.3 Conclusions

The main conclusion of this project is that the MAX phases is a unique class of intermetallic compound having a tremendous potential for applications, especially at high temperature and under hostile environment. The research described provided some of the intimate details about their structure, composition, mechanical properties and electronic structures at the fundamental level which makes this NETL supported team to be a highly visible and internationally competitive group in the world scene. The logical implication is that fundamental research based on large scale simulations should not stop here since there are many additional follow up studied needed in conjunction with experimental efforts to reach the level that tangible applications can be demonstrated.

This project is highly relevant to the NETL program under the new CrossCutting program for advanced materials research. 10 years ago, computational research was not in the main stream for NETL projects and this has been changed in recently since such effort can effectively complement the actual materials development based purely on costly trial and error and we truly believe this is the direction for future as demonstrated our genomic approach to the study of MAX phases compounds for fossil energy power system applications.

IV. GRAPHICAL MATERIALS LIST(S)

We have selected 12 graphic displays to illustrate the various tasks listed in SOPO and the accomplishments described above. Most of them can be obtained from the published literature listed in section VI. BIBLIOGRAPHY. Some of them are not in the published papers but are included in various technical reports submitted in the past.

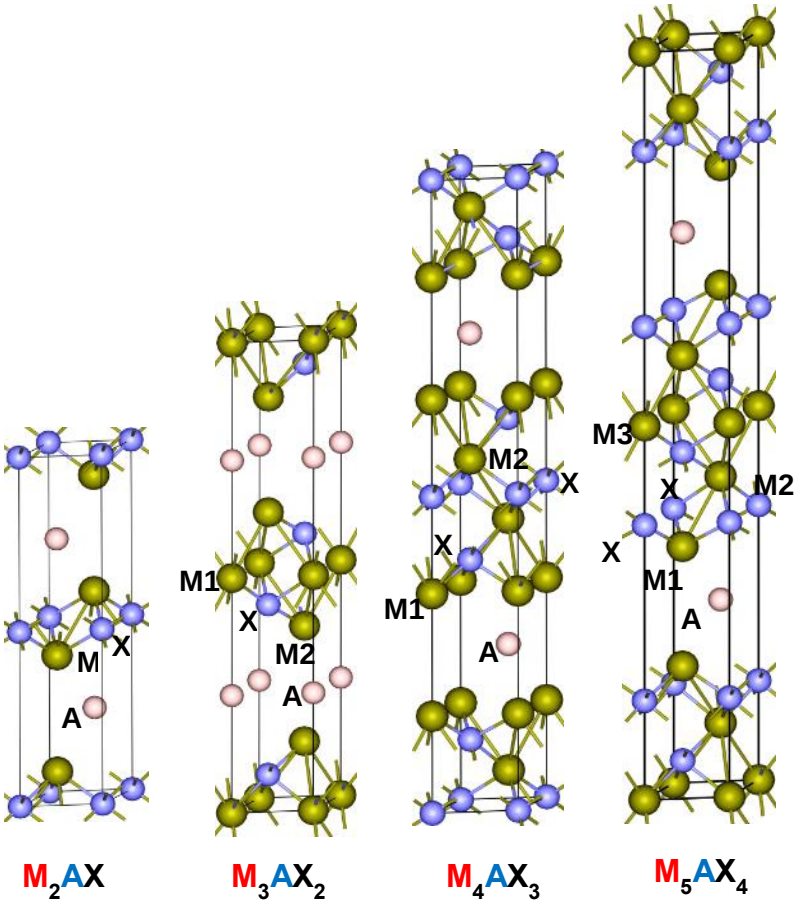

Figure 1. Sketch of crystal structures of four MAX phases M_2AX, M_3AX_2, M_4AX_3, M_5AX_4 .

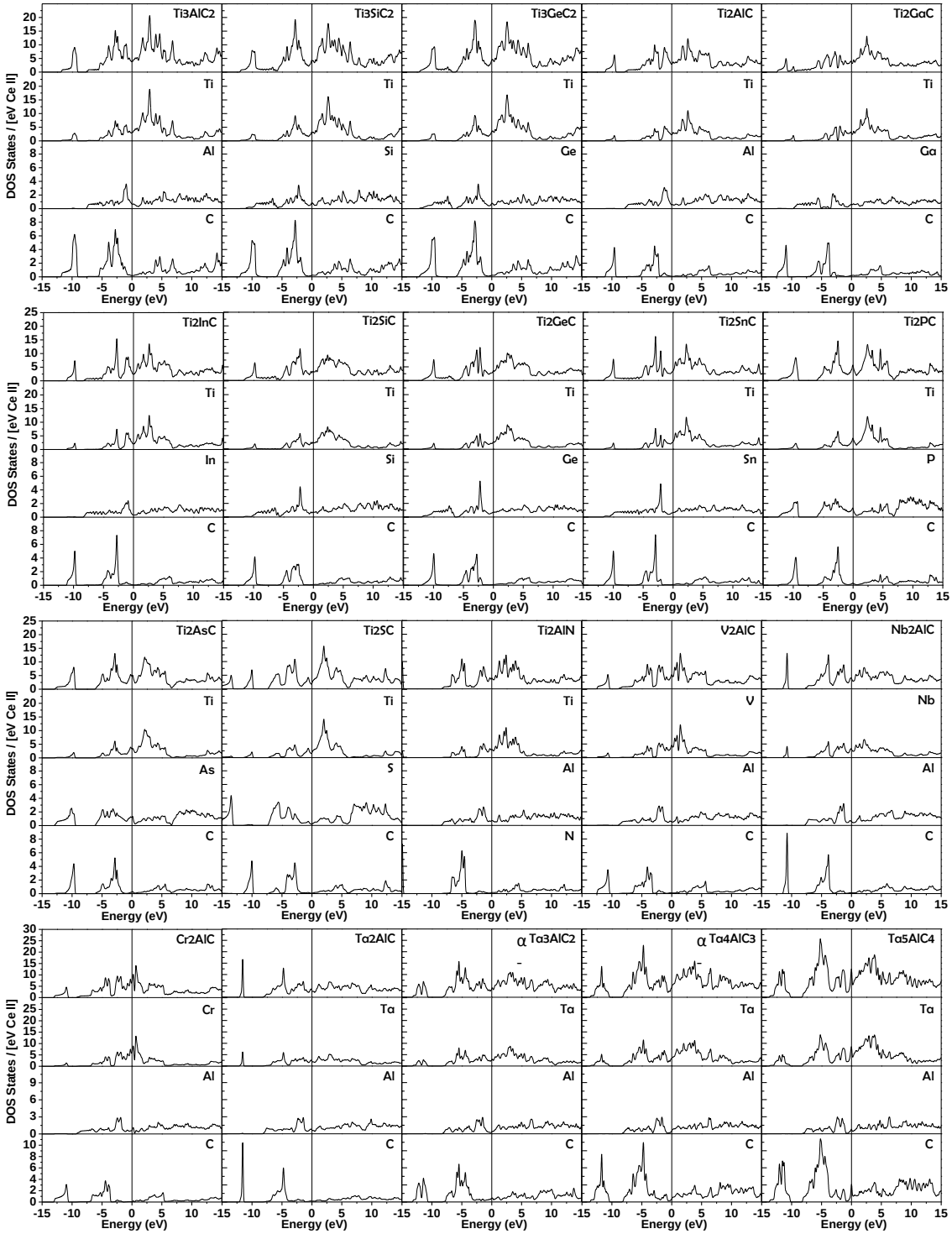

Figure 2. Calculated total and partial (atom-resolved) density of states of the 20 MAX phases.

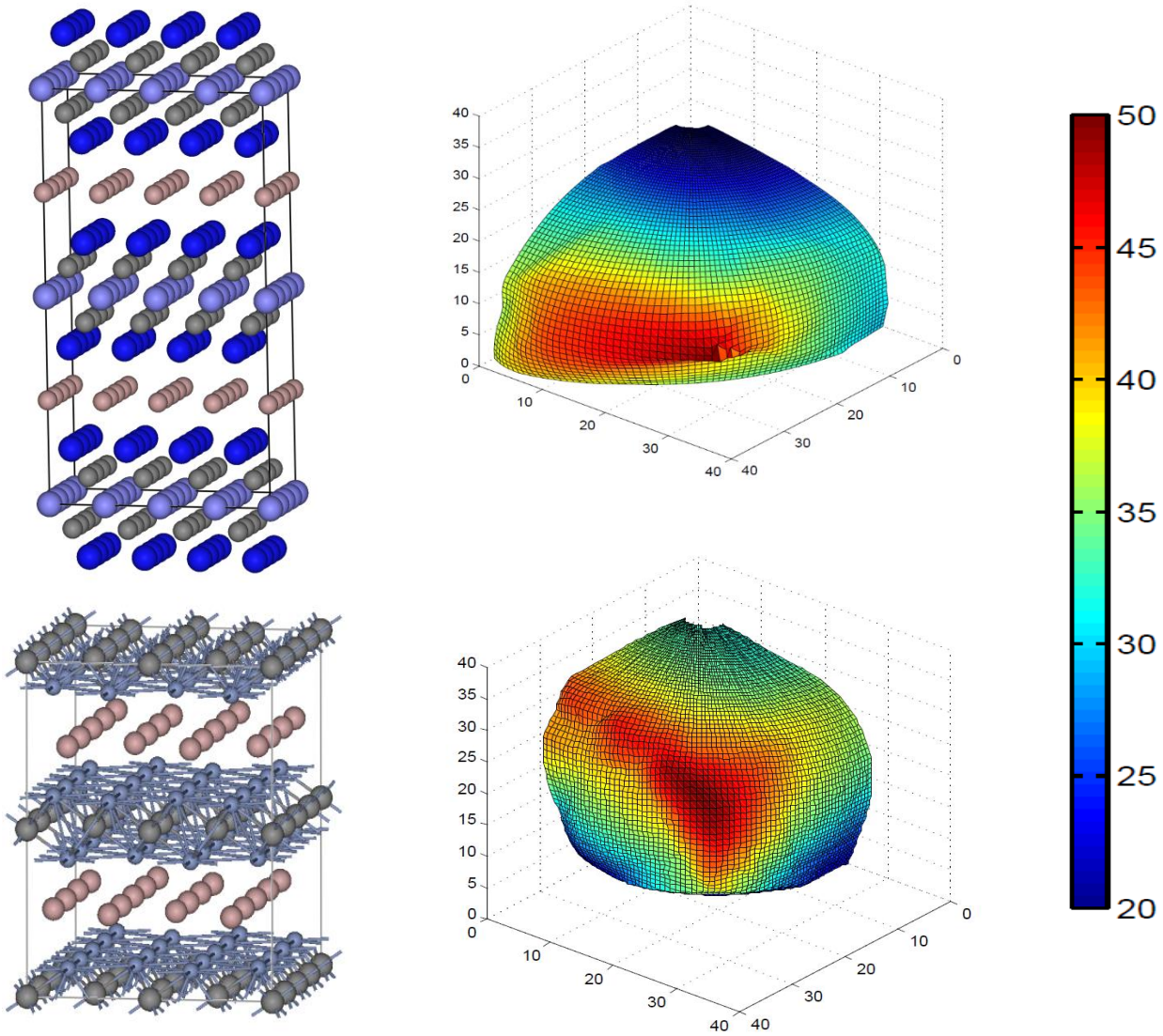

Figure 3. Supercell and failure envelope for Ti_3AlC (top) and Cr_2AlC (bottom). Unit of color bar is in GPa.

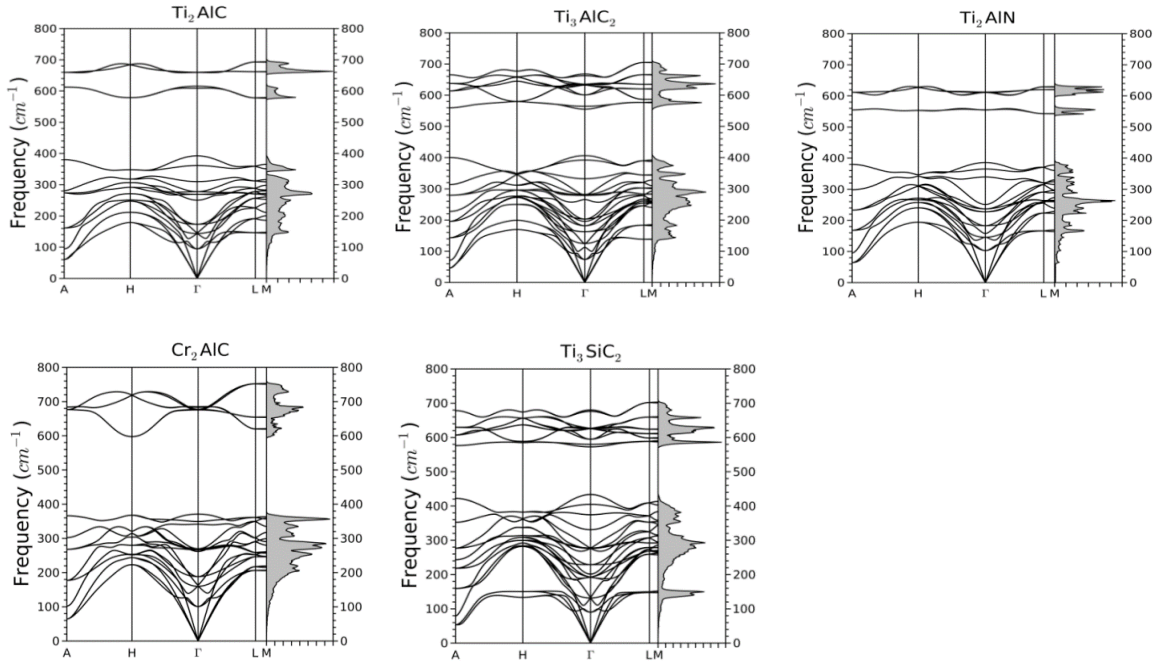

Figure 4. Calcated phonon dispersion relation and density of states for five MAX phases: Ti_2AlC, Ti_3AlC_2, Ti_2AlN, Cr_2AlC, Ti_3SiC_2.

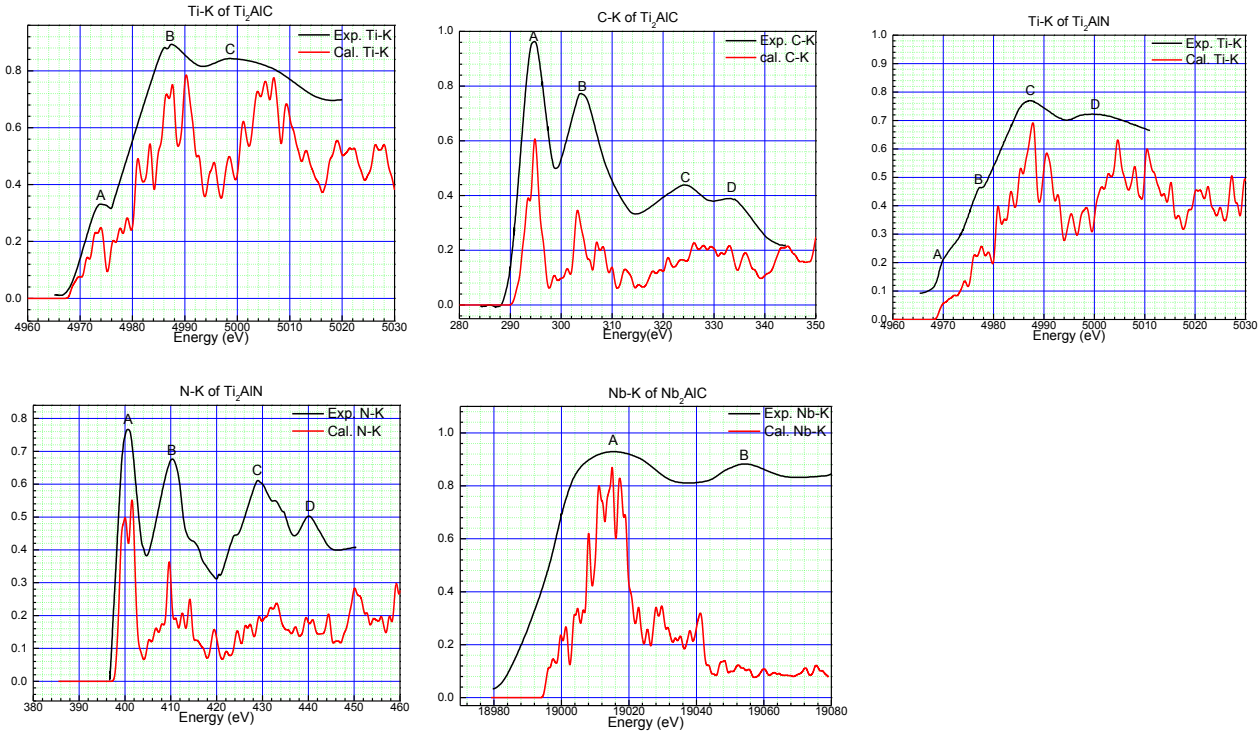

Figure 5. Comparison between experiment and calculated XANES spectra: (a) Ti-K of Ti_2AlC, (b) C-K of Ti_2AlC; (c) Ti-K of Ti_2AlN, (d) N-K of Ti_2AlN; (e) Nb-K of Nb_2AlC.

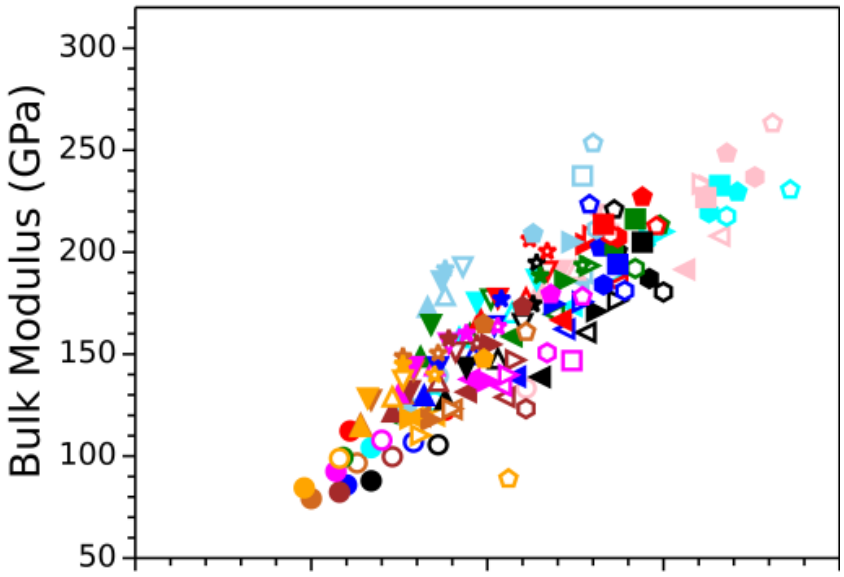

Figure 6. Correlation plots of bulk modulus K vs. total bond order density in 211 MAX phases.

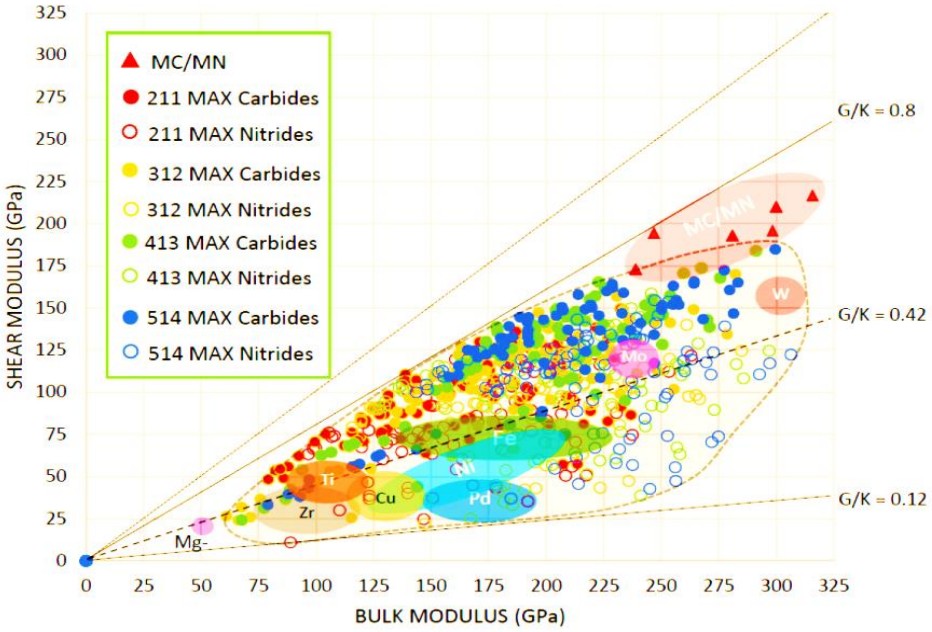

Figure 7. Shear modulus vs. bulk modulus for 665 screened MAX phases in the database. Solid circles and open circles are for carbides and nitrides respectively. Different color is used for different n in $M_{n+1}AX_n$. Also shown are the locations of other metals and binary MC and MN compounds.

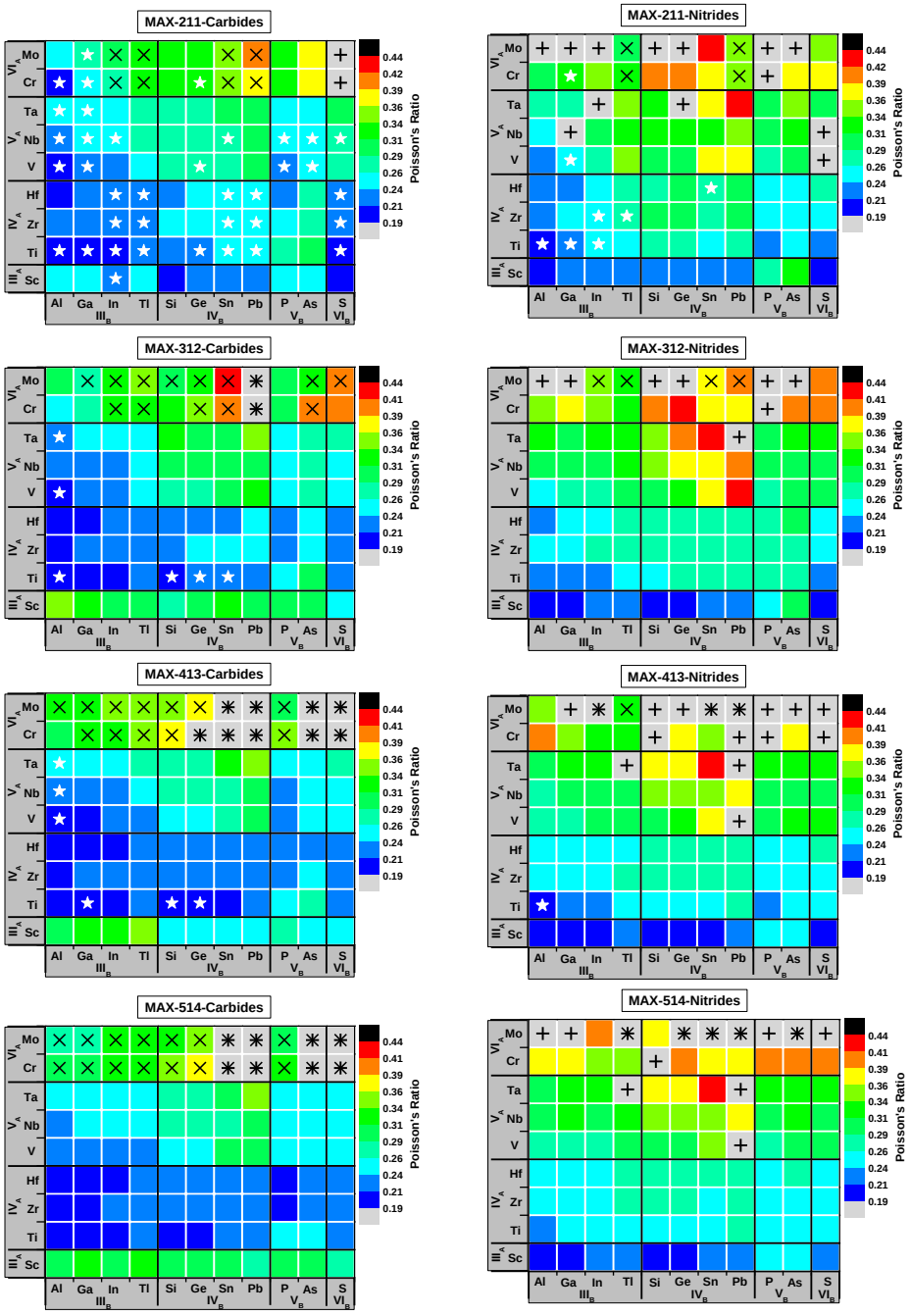

Figure 8. Poisson's ratio maps for all the MAX phases according to M (Y-axis) and A (X-axis) elements. Left column for carbides and right column for nitrides. Color in the box represents calculated G/K values as indicated in the color bar. Stars in the box indicate this phase has been synthesized. The sign + stands for elastic instability and the × sign indicates the phase is screened out for thermodynamic instability due to positive heat of formation.

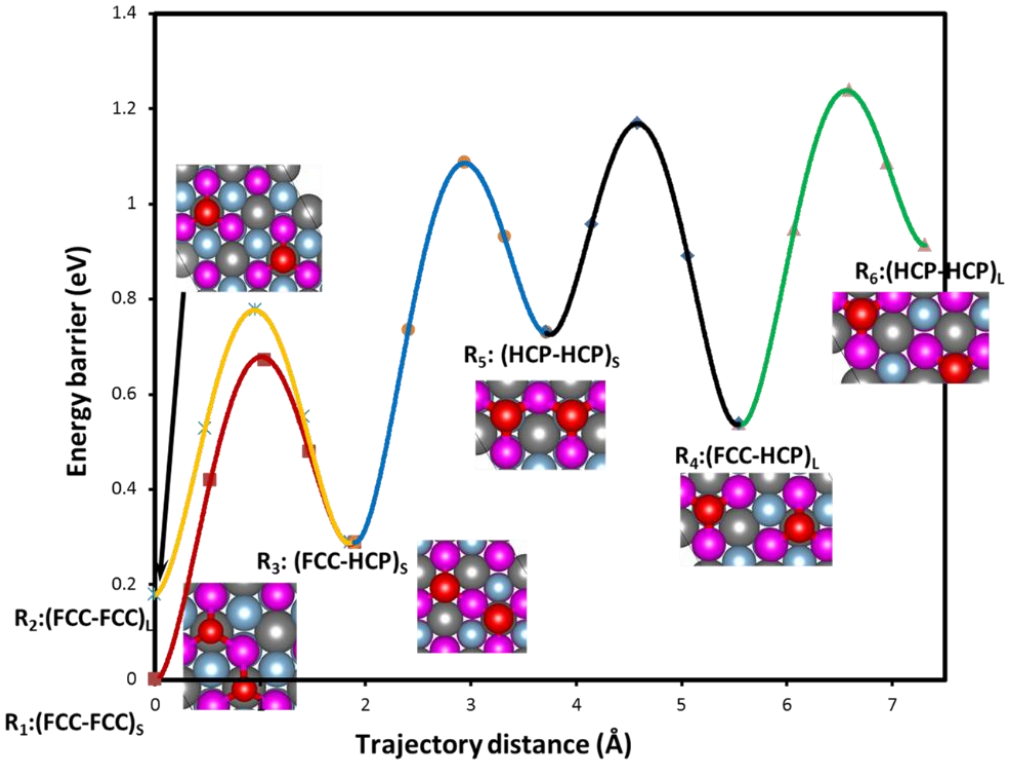

Figure 9. Six configurations of an oxygen molecule being adsorbed onto the (0 0 0 1) Al surface with the corresponding energy barriers to migrate into the adjacent con-figuration. A short-range cluster of alumina oxide with both oxygen atoms which are positioned on the FCC site is the most preferred site (R1).

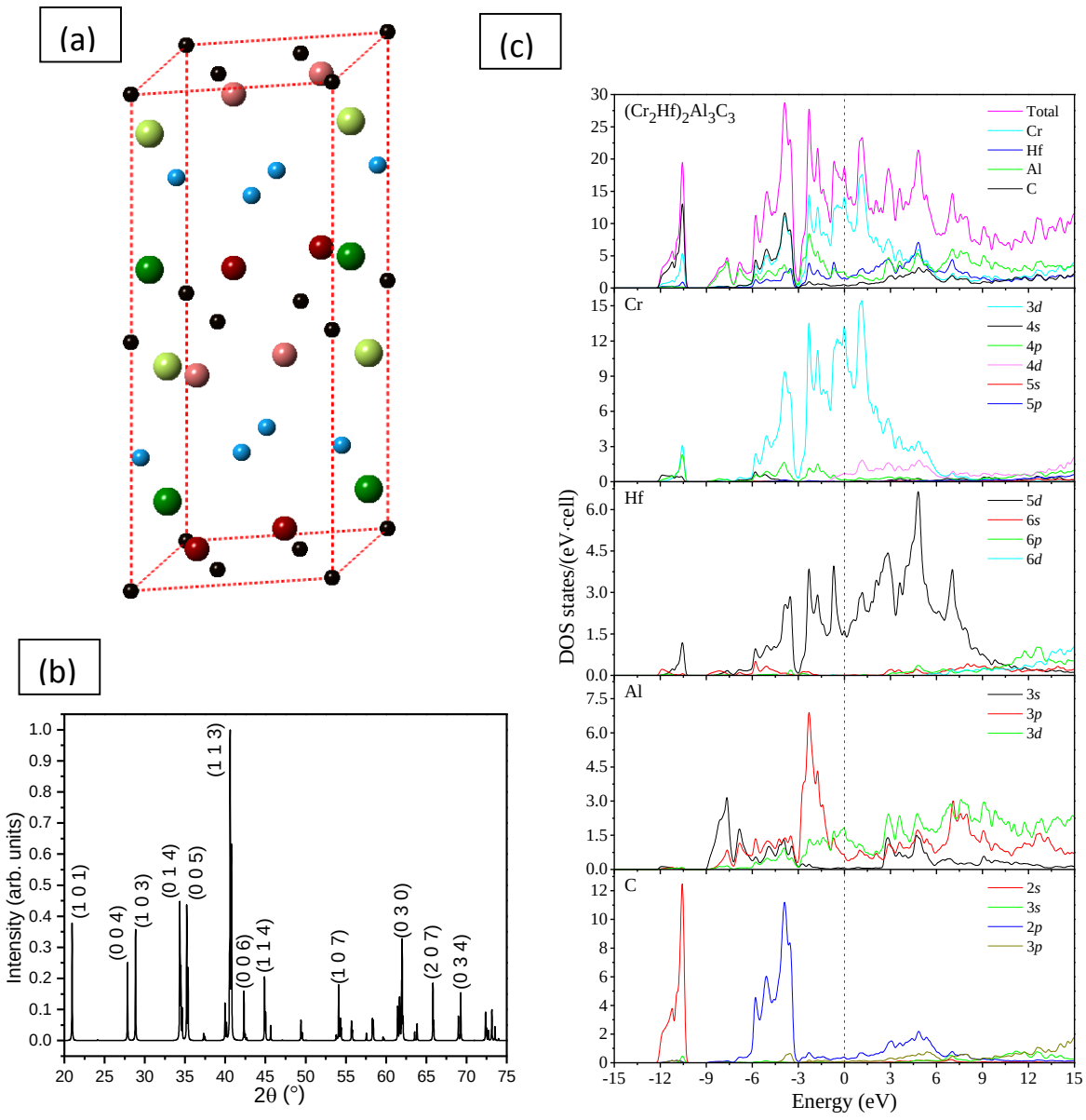

Figure 10. (a) Crystal structure, (b) Indexed x-ray diffraction pattern and (c) Total and partial DOS of $(Cr_2Hf)_2Al_3C_3$.

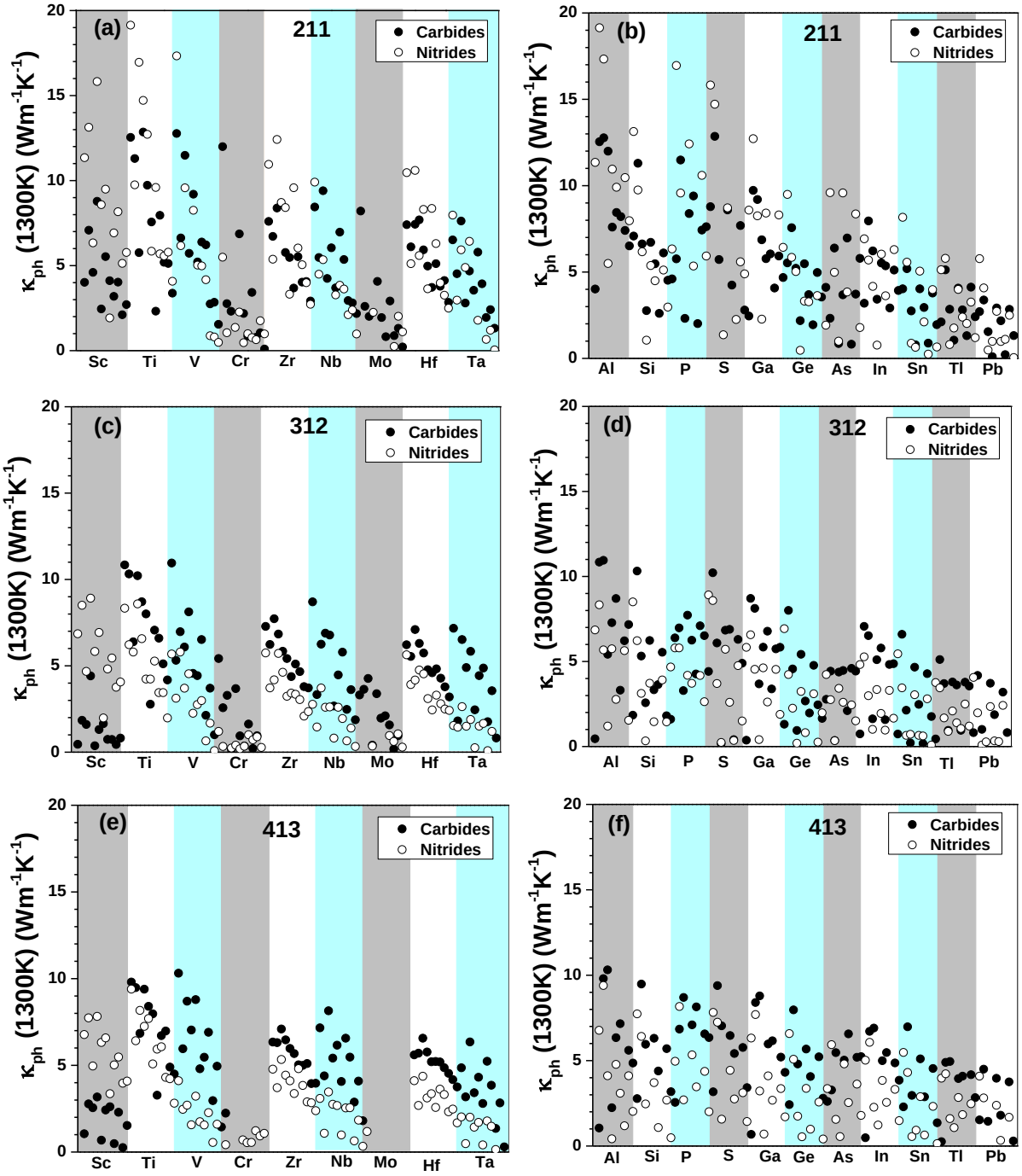

Figure 11. Scatter plots of calculated phonon thermal conductivity (κ_{ph}) at 1300K of MAX phases: (a) 211 in "M" trend; (b) 211 in "A" trend; (c) 312 in "M" trend; (d) 312 in "A" trend; (e) 413 in "M" trend, (f) 413 in "A" trend. The trend for "M" elements (Sc, Ti, V, Cr, Zr, Nb, Mo, Hf and Ta) and "A" elements (Al, Si, P, S, Ga, Ge, As, In, Sn, Tl and Pb) are along the x-axis in upper and lower panels, respectively. Each differently colored subpanel contains 22 and 18 MAX phases for the top and bottom respectively.

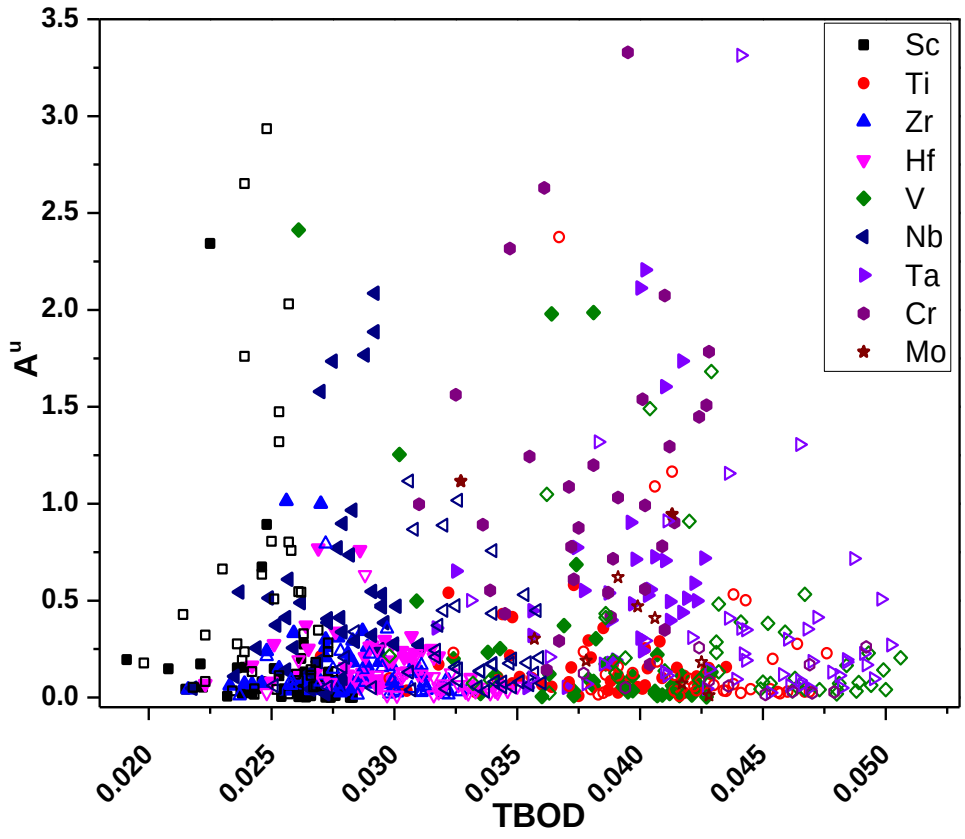

Figure 12. Universal elastic anisotropy (A^U) vs. total bond order density (TBOD) for 665 MAX carbides and nitrides in the database. There is evidence of a bimodal distribution with a minimum in A^U corresponding to a TBOD near 0.035.

V. REFERENCES

No specific Bibliography for the report is enclosed here. They can be find in each of the published paper listed in the REFERENCES Section above.

VI. BIBLIOGRAPHY

Papers published and submitted acknowledging the support from this grant. A few of the published work is only tangentially related to the project in terms of student training and method development and not specifically on the MAX phases.

Published or submitted:

1. S. Aryal, Paul, Rulis, L. Ouyang, and **W.Y. Ching**, "Structure and properties of the low-density phase ι-Al_2O_3 from first principles", Phys. Rev. B84, 174123-1-12. (2011).
2. Wai-Yim Ching, Paul, Rulis, S. Aryal, Yuxiang Mo and Lizhi Ouyang, "Large scale simulations of the mechanical properties of layered transition metal ternary compounds for fossil energy power system applications", Conference Proceedings, 2011 Advanced Research Fossil Energy Materials Conference, April 26-28, Pittsburgh, PA, (2011)
3. S. Aryal, Paul, Rulis, **W.Y. Ching**, "Mechanical Properties and Electronic Structure of Mullite Phases using First-Principles Modeling". J. Amer. Ceram. Soc. 95 [7] 2075 (Feature Article) (2012).
4. Wai-Yim Ching, Paul, Rulis, S. Aryal, Yuxiang Mo and Lizhi Ouyang, "Electronic structure and mechanical properties of 20 MAX phases compounds", Conference Proceedings, 2012 26th Annual Conference on Fossil Energy Materials Conference, April 17-19, Pittsburgh, PA, (2012)
5. Yuxiang Mo, Paul Rulis, **W.Y. Ching**, "Electronic Structure and Optical Conductivities of 20 MAX-Phase Compounds", Phys. Rev. B86, 165122-1-10 (2012).
6. A. Misra and **W.Y. Ching**. "*Ab initio* multi-axial tensile stress-strain-failure behavior of crystalline hydroxyapatite". Scientific Report, #:1488 (2013). DOI:10.1038/srep1488
7. **W.Y. Ching,** Yuxiang Mo, Sitaram Aryal and Paul Rulis, "Intrinsic mechanical properties of 20 MAX phase compounds", J. Amer. Ceram. Soc. 1-6 (2013) 3231. DOI:10.111/jace.12376
8. Liaoyuan Wang, Paul Rulis, **W. Y. Ching**, "Calculation of core-level excitation in some MAX phase compounds", J. Appl. Phys. 114, 023708 (2013). doi: 10.1063/ 1.4813221(2013).
9. Neng Li, C. C. Dharamawardhana, K.L. Yao and **W.Y. Ching**,"Theoretical characterization on intrinsic ferromagnetic phase in nanoscale laminated Cr_2GeC". Solid State Communication,174, 43–45 (2013).
10. Neng Li, R. Sakidja and **W.Y. Ching,** "Oxidation of Cr2AlC (0001): "Insights from *ab initio* calculations", JOM, Published on line (2013). DOI: 10.1007/s11837-013-0741-x
11. Liaoyuan Wang, Yuxiang Mo, Paul Rulis, and **W. Y. Ching,** "Spectroscopic Properties of Crystalline Elemental Boron and Implications on B11C-CBC", (2013). RSC Adv., 3(47), 25374-387, (DOI:10.1039/C3RA44586K
12. Yuxiang Mo, S. Aryal, Paul Rulis and **W.Y. Ching**, "Crystal Structure and Elastic Properties

of Hypothesized MAX Phase-Like Compound $(Cr_2Hf)_2Al_3C_3$", J. Amer. Ceram. Soc. ,Vol 97 [8] 2646–2653, (2014), DOI:10.1111/jace.12987.

13. S. Aryal, Ridwan Sakidja, M. Barsoum and **W.Y. Ching**, "A Genomic Approach to the Stability, Elastic and Electronic Properties of the MAX Phases", Phys. Status Solidi B, 251, No. 8, 1480–1497 (2014) / DOI 10.1002/pssb.201451226
14. Neng Li, R. Sakidja and **W.Y. Ching,** "Ab Initio studies on the absorption mechanism of oxygen on Cr_2AlC (0001) Surface", Applied Surface Science, 315, 45-54 (2014).
15. S. Aryal, R. Sakidja, L. Ouyang, **W.Y. Ching**, "Elastic and Electronic Properties of $Ti_2Al(C_{1-x}N_x)$ Solid Solutions", Accepted by J. Eur. Ceramic. Soc. (in press, 2015).
16. C. Dhakal, R. Sakidja, S. Aryal and **W.Y. Ching**, "Calculation of Lattice Thermal Conductivity of MAX Phases", submitted to J. Eur. Ceramic. Soc. (2015).
17. S. Aryal, K. Matsunaga, and **W- Y. Ching,** "Elastic and mechanical properties of Zn and Mg doped Hydroxyapatite (HAP) Crystals", submitted to J. Mechanical Behavior of Biomedical Materials. (Accepted, 2015)
18. **Wai-Yim Ching**, "Materials Informatics using *Ab initio* Data: Application to MAX Phases ", in "Information-driven approach to materials discovery and design", Springer Materials Series. Editors: Turab Lookman, Frank Alexander and Krishna Rajan. (2015).

<u>To be submitted at a later time</u>:

19. C. C. Dharamawardhana and **W. Y. Ching**," Universal Elastic Anisotropy all MAX phases", to be submitted to J. Amer. Ceramic Soc.

VII. APENDICES

A book chapter written for the book "Information-driven approach to materials discovery and design", Springer Materials Series. Editors: Turab Lookman, Frank Alexander and Krishna Rajan. (2015) is enclosed.

Materials Informatics using *Ab initio* Data: Application to MAX Phases

Wai-Yim Ching

Abstract

We use a database that was constructed for a very unique class of laminated intermetallic compounds, the MAX ($M_{n+1}AX_n$) phase, to show how materials informatics can be used to predict the existence of new, hitherto unexplored phases. The focus of this Chapter is the correlation between seemingly disconnected descriptors and the importance of high quality, computationally derived data. An extension of this approach to other specific materials systems is discussed.

1. Introduction.

In recent years, information gathering, analysis, and interpretation has emerged as an interdisciplinary research skill involving computer science, information science, and other various domains of science such as physics, chemistry, biology, medicine, materials engineering, design technology, education and social science, *etc*. [1]. In particular, materials informatics has developed into a flourishing field of study [2]. It aims to find more efficient ways of solving scientific problems related to all kinds on materials using large databases. This started at the initiation of the materials genome project at the federal level and it follows the same approach that the Human Genome Project in the biomedical community did decades ago, which resulted in the now mature discipline of bioinformatics. Creative software, genetic algorithms, and visualization tools have been developed to do statistical analysis of data and to explore the data via data mining aided by powerful high performance computers [3]. There are many examples of highly successful applications for identifying and understanding the structure-properties correlations and to formulate design rules for better materials for specific applications. The information obtained from high throughput materials informatics greatly reduces the time that it takes to go from frontier research to real applications.

There are many different ways of collecting large data and of building powerful databases for applications. Traditionally, the data for materials properties are collected from experimentally measured values published in open literature such as: crystal structures, density, heat of formations, melting temperature, electric conductivity, thermal conductivity, refractive index, bulk modulus, hardness, phase diagrams, and much more. These data cover all kinds of material systems regardless of the source or the reliability of the data. Such database are usually not vetted and they are of varying quality. However, the argument is that in a statistical sense, any invalid data that appears does so as noise and will not make much of a difference, as long as the database is large enough and the method for analysis is carefully designed. This *modus operandi* is more common in the biomedical arena when dealing with experimental or clinical trials with large data collected over a long period of time while looking for small effects [4]. Contrary to some approaches which aim to reduce or avoid accurate atomistic simulations by instead relying purely on statistical predictions, is another approach that is based on the design of a specific data base with high

accuracy using computational genomics. This difference simply reflects the emphasis on a different spectrum of the field of materials informatics with different strategies for different systems although both are data driven.

More recently, large amounts of data may be obtained through calculations using different computational methods and packages based on different theories. The trend is usually to cover a focused groups of materials that are categorized either in their structure, composition, functionality, or some specific materials property. Examples for such recent endeavors include: piezoelectric perovskites [5], battery materials comprising oxides, phosphates, borates, silicates sulphates, etc.[3]; [6], Half-Heusler semiconductors with low thermoconductivity [7], binary compounds [8], polymer physics materials genome [9], and isotope substitution on phonons in graphene [10] just to name a few. It is also possible to combine the measured data and the calculated data into a bigger database.

In this Chapter, we present a specific case to illustrate the application of materials informatics using a large database of a unique class of materials, the MAX ($M_{n+1}AX_n$) phase [11]. Our approach is to select a specific material system with well-defined structures and compositions for a focused study and then apply state-of-the art computational tools to systematically generate a large amount of data on their physical properties, and the analysis of correlations amongst them. We then use this database to test the efficacy of exiting data mining and machine learning algorithms. Simultaneously, this enables us to predict the existence of new MAX phases that have not yet been synthesized or studied in the laboratory but which may have outstanding properties. The identification of outliers that clearly do not follow general trends helps to obtain deeper insights and reveal the fundamental reasons behind such deviations. The predictive capability of the data mining is substantially controlled by the quality of the assigned descriptors. At the same time, use of theoretical-based descriptors that demand a large computational time will be impractical. Thus, delegating such types of descriptors to a combinations of less time-demanding descriptors will be the goal. This approach is certainly different from other approaches which depend on collecting data from various sources but it puts the data under better control with increased reliability in the interpretations.

Another important issue which is less frequently discussed in materials informatics is the way that the data are presented. Many believe that materials informatics relies on massive data collections and their statistical analysis. Everything is numerical and machine-based. On the other hand, we find that creative and insightful graphical representations of the data can allow one to grasp some of the most important points without laborious analysis. This will be amply demonstrated for the materials presented in this Chapter.

The MAX phase is used as an example to illustrate various aspects of materials properties and correlations between different descriptors. We have identified one such descriptor in particular, the total bond order density (TBOD) that plays a dominating role. We articulate on some other materials systems for which the application of the same approach and the use of TBOD can be very fruitful.

2. MAX Phases: A unique class of material

MAX phases or $M_{n+1}AX_n$ are transition metal ternary compounds with layered structures where "M" is an early transition metal, "A" is a metalloid element, "X" is either carbon or nitrogen, and n is the layer index. MAX compounds have attracted a great deal of attention in recent decades due to many of their fascinating properties and wide range of potential applications. Up to now, only about 70 of these phases are confirmed or have been synthesized [12]. The majority of these confirmed phases are 211 carbides with n = 1 or 2 and with M = Ti and Zr, and A = Al and Ga. It has also been demonstrated that the formation of composite phases and solid solutions in MAX phases between different "M" elements, "A" elements and C and N are possible. Such possibilities have greatly extended the range of compositions beyond the ternary phases.

The MAX phases are layered hexagonal crystals (space group: $P6_3/mmc$ No. 194). **Figure 1** displays the crystal structure of MAX for n = 1, 2, 3, 4, which are usually referred to as the 211, 312, 413, and 514 phases. An important feature is that in MAX compounds, layer "A" remains constant whereas layers of "M" and "X" increase with n. The "X" layers are always in between the "M" layers or blocks of MX layers connected by single "A" layer which can significantly affect the properties of a MAX phase. The physical properties of MAX phases vary over a wide range depending on "M", "A", "X" and n. MAX phases with $n \geq 5$ are known to exist but are very rare. Most of the existing experimental work on the MAX phases has been on the 211 and 312 carbides.

MAX phases behave both like ceramics and metals with some very desirable properties such as machinability, thermal shock resistance, damage tolerance, fatigue, creep, and oxidation resistance and elastic stiffness. They are also good thermal and electrical conductors [12]. More recently, MAX phases have been considered for high-temperature structural applications. Other applications include porous exhaust gas filters for automobiles, heat exchangers, heating elements, wear and corrosion protective surface coatings, electrodes, resistors, capacitors, rotating electrical contacts, nuclear applications, as bio-compatible materials, cutting tools, nozzles, tools for die pressing, impact-resistant materials, projectile proof armor, and much more. Some of these applications already have products on the market.

The physical properties of MAX phases have been investigated by many groups both experimentally and computationally (See extensive references in Aryal *et. al.* [11]). We have been focusing mostly on the mechanical properties and electronic structure of MAX phases. The elastic coefficients and mechanical parameters such as the bulk modulus (K), shear modulus (G), Young's modulus (E), and Poisson's ratio (η) are derived from the calculated elastic coefficients under the VRH polycrystalline approximation and were obtained. The G/K ratio, also known as the Pugh moduli ratio is a good indicator of the ductility or brittleness of the alloy based on an analysis in pure metals but it has also been quite effective when applied to metallic alloys [13] . The other physical properties investigated are the optical conductivities in 20 MAX phases [14] and the core-level excitations in some of the compounds [15]. More recently, we also estimated the high temperature lattice thermal conductivities of MAX phases (see Section 4).

The electronic structure and bonding is the basic information needed to understand the properties in any materials. It has been well studied for MAX phases using density functional theory-based methods by many groups over the last 15 years. Most of the discussion tends to be on the band structure and the density of states (DOS) and partial density of states (PDOS). In MAX phases, interatomic bonding are fairly complicated involving metallic, partly covalent and partly ionic types of bonding which may extend beyond nearest neighbors. The structural complexity and variations in chemical species make characterization of interatomic bonding in MAX phases particularly challenging. We advocate the use of total bond order (TBO), total bond order density (TBOD) and their partial components (PBOD) as useful metrics to delineate the observed physical properties. TBO is the sum of all bond order pairs in the crystal and when normalized by its volume, we get the TBOD. This will be illustrated more in the following sections.

It is worth mentioning that in addition to the canonical MAX phases, there are related materials derived from the MAX phases such as the solid solutions with different "M" or "A" elements and with mixtures of C and N. The MAX solid solutions can expand the list of such compounds enormously and some of them may have optimized compositions that enhance their properties. This provided a great opportunity to apply the techniques of materials informatics for facilitating the processing of large amounts of data. Other related systems include the 2-dimentional $M_{n+1}X_n$ system called Maxenes by extracting the "A" layer from MAX by exfoliating in solution which offers a variety of new applications. Last but not least, there are quite a few layered intermetallic compounds with different types of stacking layers but involving more or less similar chemical species that have not been fully exploited.

3. Applications of materials informatics to MAX phases

3.1 Initial screening and construction of the MAX database

We first construct a database consisting of as many MAX phases in accordance with the general guideline suggested by Barsoum (Barsoum's Book, page 2, Fig. 1.2 [12]). We chose 9 "M" elements (Sc, Ti, Zr, H, V, Nb, Ta, Cr, Mo), 11 "A" elements (Al, Ga, In, Tl, Si, Ge, Sn, Pb, P, As, S), X = C and N and with the layer index n = 1,2,3,4. This gives us a total of 792 possible MAX ($M_{n+1}AX_n$) phases. We used the Vienna *Ab initio* Simulation Package (VASP) [16] to optimize the structure and obtain the elastic constants for each crystal. However, not all of these phases will be stable. We therefore screen these by using two stability criteria: the Cauchy-Born elastic stability criteria for hexagonal crystals [17] which eliminated 71 crystals. Next, we calculated the heat of formation (HoF) for the same 792 crystals based on the relative stability of each MAX phase to the formation energy of its elements in their most stable ground state structure. As a result, 45 additional phases with positive HoF were eliminated, resulting in 665 viable MAX phases for a more focused study. The use of these two criteria instead of a more rigorous but far more time consuming one based on thermodynamic assessment on all potential competing phases in the M-A-X ternary phase diagrams is a reasonable compromise. In principle, we can consider these two sets of criteria employed as two descriptors in the data mining approach. This represents a substantial savings in computational time. The calculated elastic and mechanical properties of the 665 MAX phases are tabulated as illustrated in **Table I** for 20 such phases. The electronic structure and bonding of the MAX phases are calculated using the orthogonalized linear

combination of atomic orbital method (OLCAO) [18]. This is an extremely efficient and well-tested method using atomic orbitals in the basis expansion. The main descriptors for electronic properties are summarized in tabular form as illustrated in **Table II** for 14 such crystals. Both sets of data for the 665 MAX phases are publically available [11].

Table I. Samples of descriptors for mechanical properties in the database (Units in GPA)

Crystals	C_{11}	C_{12}	C_{13}	C_{33}	C_{44}	C_{66}	K	G	E	η	G/K
Ti_3AlC_2	355.8	81.4	75.3	293.4	120.3	137.2	162.5	126.7	301.7	0.191	0.78
Ti_3SiC_2	369.6	96.2	107.6	358.3	155.0	136.7	191.1	141.3	340.0	0.204	0.74
Ti_3GeC_2	362.0	97.2	97.7	332.0	137.3	132.4	182.2	132.2	319.3	0.208	0.73
Ti_2AlC	301.9	68.0	63.0	267.9	105.1	117.0	139.7	110.5	262.3	0.187	0.79
Ti_2GaC	300.8	79.2	63.8	246.5	92.4	110.8	139.3	101.4	244.9	0.207	0.73
Ti_2InC	284.4	69.3	55.2	235.5	83.9	107.5	128.6	96.0	230.5	0.201	0.75
Ti_2SiC	312.9	82.1	110.4	329.2	149.6	115.4	173.0	124.9	302.0	0.209	0.72
Ti_2GeC	296.6	85.7	96.8	297.1	121.5	105.5	161.0	110.0	268.8	0.222	0.68
Ti_2SnC	262.6	88.6	73.1	255.2	96.8	87.0	138.8	92.4	226.8	0.228	0.67
Ti_2PC	256.8	144.8	155.0	339.5	166.3	56.0	191.8	93.1	240.4	0.291	0.49
Ti_2AsC	212.9	180.4	123.7	289.5	146.3	16.2	150.7	57.2	152.3	0.332	0.38
Ti_2SC	339.8	101.4	109.7	361.9	159.5	119.2	186.8	134.4	325.2	0.210	0.72
Ti_2AlN	312.9	73.0	95.5	290.7	126.1	120.0	160.5	117.4	283.1	0.206	0.73
V_2AlC	334.4	71.5	106.0	320.8	149.8	131.5	172.9	132.1	315.9	0.196	0.76
Nb_2AlC	316.6	86.3	117.0	288.6	137.6	115.2	173.6	116.4	285.5	0.226	0.67
Cr_2AlC	366.3	85.8	111.3	356.9	142.9	140.2	189.6	137.0	331.2	0.209	0.72
Ta_2AlC	344.5	112.2	137.1	327.9	152.3	116.1	198.8	124.1	308.1	0.242	0.62
α-Ta_3AlC_2	453.6	130.5	135.6	388.4	175.0	161.5	232.8	161.1	392.8	0.219	0.69
α-Ta_4AlC_3	459.2	149.1	148.7	383.1	170.5	155.0	243.0	155.3	384.1	0.237	0.64
Ta_5AlC_4	481.5	149.6	158.1	423.6	188.8	165.9	257.2	169.1	416.0	0.231	0.66

Table II. Samples of descriptors from electronic structure in the database. ΔQ* and bond orders (electrons) and $N(E_F)$ (states/eV-cell).

MAX	ΔQ*(M)	ΔQ*(X)	ΔQ*(A)	TBO	BO(M-X)	BO(M-M)	BO(M-A)	BO(A-A)	$N(E_F)$
Ti_2AlC	-0.330	-0.043	0.703	23.510	10.258	4.512	7.231	1.508	11.052
Ti_2GaC	-0.485	0.269	0.701	22.680	10.289	4.060	6.986	1.340	10.572
Ti_2InC	-0.424	0.148	0.700	22.750	10.238	4.396	6.482	1.636	9.260
Ti_2SiC	-0.393	0.097	0.688	22.820	10.344	3.583	8.153	0.742	12.921
Ti_2GeC	-0.509	0.324	0.694	21.750	10.337	3.541	7.111	0.758	14.720
Ti_2SnC	-0.381	0.069	0.693	22.320	10.294	3.926	7.110	0.993	15.084
Ti_2PC	-0.454	0.210	0.699	22.740	10.366	2.802	9.571	0.000	21.762
Ti_2AsC	-0.505	0.316	0.695	21.360	10.382	2.893	8.086	0.000	19.697
Ti_2SC	-0.447	0.189	0.705	21.340	10.380	2.944	8.018	0.000	7.301
Ti_2AlN	-0.295	-0.087	0.679	22.150	8.702	4.646	7.217	1.585	15.502
V_2AlC	-0.277	-0.101	0.655	22.820	10.017	4.192	6.905	1.704	21.663
Nb_2AlC	-0.493	0.245	0.741	15.410	7.319	1.253	5.354	1.399	13.338
Cr_2AlC	-0.098	-0.324	0.521	21.250	9.559	2.837	7.080	1.769	24.384
Ta_2AlC	-0.324	-0.044	0.692	24.810	10.130	5.724	7.561	1.397	11.126

3.2 Representative results on mechanical properties and electronic structure of MAX phases.

We selectively present some of the calculated results from the database for the 665 MAX phases. **Figure 2** shows a scattered plot of shear modulus G vs. bulk modulus K for all screened 665 MAX phases. To have a broader perspective, we used different colors for index n, and open or closed symbols for carbides and nitrides respectively. We also include similar data for some metallic compounds and selected binary MX compounds [19]. We note that the MAX phases cover a wide region of bulk and shear moduli, overlapping with those of the common metals and alloys. The dashed lines show the G/K ratios for these data which range from a minimum of 0.12 to a maximum of 0.8. The maximum G/K ratio is close to those of MN binary compounds and the low G/K values are mostly from MAX nitrides. **Figure 2** illustrates a conventional graphical presentation in materials informatics to provide an overview of the data from a large database.

The data for G/K values for all MAX phases shown in **Figure 2** as scattered plot data are presented in **Figure 3** in a different way in the form of an innovative map resembling the Periodic Table. For this plot we used the original 792 hypothetical MAX phase data**.** This enables us to clearly see the locations of those phases that have been screened out relative to those that have not. Here the "M" elements are plotted on the Y-axes and the "A" elements are along the X-axes. The color of each square cell represents the G/K value of that particular MAX phase along with other information such as whether the phase has been synthesized or not. The phases that have been eliminated by the Cauchy-Born criterion or the HoF criteria are marked with a + or a × respectively. The experimentally confirmed phases are marked with a white star. As can be seen, none of the experimentally confirmed phases are among the ones judged to be unstable and screened out. There are many boxes of different colors without the white star, suggesting the existence of a myriad of possible MAX phases not yet explored. While the G/K ratio of MAX phases can vary over a wide range as indicated by the variations in color for the different squares in **Figure 3**, we can delineate the boundaries of MAX's materials properties within which optimized functionalities can be further explored. Similar maps for other mechanical properties for the MAX phases can be found in ref. [11]

We now present some of the results related to electronic structure. The density of states (DOS) at the Fermi level (E_F) or $N(E_F)$ is one of the important electronic parameter for metallic systems. In MAX phases $N(E_F)$ is a strong function of composition. Some values are close to zero, whereas others are quite large, depending on whether E_F is located in the vicinity of the 3d or 4d orbitals of "M". The calculated $N(E_F)$ per unit cell is found to be reasonably correlated with the total valance electron number per volume (N_{val} ($Å^{-3}$) as shown in **Figure 4**. The total valance electron number is the sum of the formal valance electrons of individual atoms in the crystal. In general, larger N_{val} ($Å^{-3}$) corresponds to larger $N(E_F)$ as expected. Also, as n increases, N_{val} ($Å^{-3}$) increases, the slope of the data distribution decreases. Traditionally, it has been speculated but not rigorously proved that the existence of a local minimum (or pseudo gap) at the Fermi level in a metal or alloy signifies its structural stability [20]. While all the DOS for the MAX phases are available, it is not practical to present the DOS figures for all the phases. However, the relative magnitudes of $N(E_F)$ and its decomposition into different atomic components for each phase is a valid descriptor for the electronic structure.

Figure 4 shows that nitrides have larger $N(E_F)$ values than the carbides. The Sc-based carbides, however, are a notable exception. They have significantly higher $N(E_F)$ than their nitride counterparts. The Sc-based carbides (but not the nitrides) also show a marked deviation from the general trend of $N(E_F)$ vs. N_{val} ($Å^{-3}$) with increasing n. The approximate positive linear correlation between the two properties becomes more pronounced with increasing n which can be attributed to the increased M atoms as n increases. One can relate this linear trend to a similar behavior observed in the binary mono-carbides or nitrides [21]. However, a real distinction here with respect to the MAX phases is the profound role of "A" which is not present in the binary mono-carbides/nitrides. In general, the presence of the "A" element appears to significantly lessen the degree of the linear correlation or increase in the scattering of the data (see **Fig. 4** for MAX 211). It is only at higher n values, where the "A" content is reduced and consequently the bonding characteristics are less influenced by "A", that a stronger correlation between the two properties emerges, mimicking those of binary mono- carbides/nitrides.

3.3 Classification of descriptors from the database and correlation among them

The MAX database consists of the calculated quantities of all MAX phases as illustrated in **Table I** and **Table II** shown earlier. These numerical quantities can be classified into descriptors or controlling factors to be used in data mining algorithms for materials informatics and to explore their correlations. A simple flow chart is shown in **Figure 5**. For the MAX phases, we classify the descriptors into three categories based on their level complexity and/or computational time required to obtain the data:

(1) Basic chemistry descriptors: They are (i) number of valence electrons, (ii) atomic number Z of the elements, and (iii) volume of the unit cell.
(2) Descriptors from the electronic structure and bonding: They are: (i) Total bond order density (TBOD) (normalized to crystal volume), (ii) total bond order from different atomic pairs, or the M-M, M-A, M-X, A-X and X-X pairs, (iii) density of states at the Fermi level ($N(E_F)$).
(3) Descriptors for the elastic constants C_{ij} and the bulk mechanical parameters, K, G, E, η and G/K ratio.

We then seek to establish the correlations between these descriptors which are interrelated. More specifically, correlations between elastic and mechanical descriptors, correlations between electronic descriptors and correlation between mechanical descriptors and electronic descriptors [11]. We have been able to demonstrate that over 90% correlation can be achieved using a simple linear regression method implying that the mechanical properties descriptors can be adequately represented by the other two types of descriptors. This is illustrated in the following section.

3.4 Verification of the efficacy of the materials informatics tools

The success in linking the electronic structure factors to complex bulk elastic properties has enabled us to advance the utility of the data mining approach for expanding the materials database for MAX phases. We have also extended our analysis into the components of the second order elastic constants of the MAX phases. **Figure 6** shows an example of such an analysis as applied

to the 2-1-1 MAX carbides, a large subset of our database. The three main elastic constants in the database, C_{11}, C_{33}, C_{13}, which were calculated using an *ab initio* method are compared to those same values as predicted by a combination of electronic structure factors and valence electron information with reasonably high correlation coefficients of 0.83, 0.93, 0.95 respectively. This suggests that such a method is robust enough to probe orientation dependent second-order elastic constants with a high accuracy.

Result of linear regression of C_{11}, C_{33}, and C_{13} with chemical and electronic descriptors shown in **Figure 6** are as follows:

$C_{11} = 0.6235 \times Z_M + 8.1344 \times (GN)_M - 0.8737 \times Z_X + 32.0051 \times Q_A - 144.2461 \times Q_X + 10.9223 \times (BO)_{M\text{-}X} + 9.2461 \times (BO)_{M\text{-}A} - 7.8791 \times (BO)_{M\text{-}M} + 11.8688 \times (BO)_{A\text{-}A} + 470.6772 \times (BO)_{A\text{-}X} - 2.7405 \times N(E_F) + 243.5997.$
Correlation coefficient = 0.83

$C_{33} = 0.7155 \times Z_M + 19.8291 \times (GN)_M - 1.085 \times Z_X + 18.9992 \times (GN)_X + 18.4127 \times (BO)_{M\text{-}A} - 8.9407 \times (BO)_{M\text{-}M} + 16.2802 \times (BO)_{A\text{-}A} - 1.0634 \times N(E_F) + 38.8039.$
Correlation coefficient = 0.9264.

$C_{13} = 36.994 \times (GN)_M - 0.402 \times Z_X - 7.3952 \times (GN)_X + 67.8729 \times Q_A - 12.8243 \times (BO)_{M\text{-}X} + 15.916 \times (BO)_{M\text{-}A} + 7.6037 \times (BO)_{M\text{-}M} - 33.8152 \times (BO)_{A\text{-}A} - 11.1306.$
Correlation coefficient = 0.9541.

where Z_M = atomic number of M, $(GN)_M$ = group number of M from Periodic Table, Z_X = atomic number of X, $(GN)_X$ = group number of X, $(BO)_{M\text{-}A}$ = total bond order of M-A pairs, $(BO)_{M\text{-}X}$ = total bond order of M-X pairs, $(BO)_{M\text{-}M}$ = total bond order of M-M pairs, $(BO)_{A\text{-}X}$ = total bond order of A-X pairs, $(BO)_{A\text{-}A}$ = total bond order of A-A pairs, $N(E_F)$ = DOS at the Fermi level. Q_A and Q_X are the effective charges on A and X respectively. (See ref. [11] for more details).

Figure 7 and **Figure 8** show a different way to test the efficacy of the data mining algorithm. Here, we use 50% of randomly chosen data from the database as a training set and use the existing algorithm WEKA [22] to predict the properties of the other 50% of the MAX phases by comparing predicted values with the *ab initio* data in the database. **Figure 7** (top panel) shows the comparison between K obtained from *ab initio* calculations vs. those obtained from the formulas derived from the data mining algorithm for the other 50% for the 211, 312, 413 and 514 MAX phases. An excellent correlation with over 90% correlation factor for each type of the MAX phase is obtained. The lower panel of **Figure 7** also shows pie charts of the relative contribution from each type of the electronic structure descriptors used to predict K. The four most important factors are the total bond order density (TBOD), BOD of the M-A pairs (M-A BOD), BOD of the M-X pairs (M-X BOD) and charge transfer for the X elements. TBOD clearly stands out as the most important factor in determining K for all MAX phases. **Figure 8** shows a similar prediction for G/K ratio using the same procedure. Although the correlation factor is less impressive than for K, the prediction from data mining is still reasonably good, with correlation coefficients around 80% or higher. The prediction for Poisson's ratio is at the same level as for the G/K ratio. In both cases,

they are strongly affected by the TBOD although it is a negative correlation instead of the positive correlation exhibited by K. The linear correlation is less definitive in this case, which is probably due to the fact that the G/K ratio or Poisson's ratio are more influenced by the nature of the "A" element. This is an effect that apparently is not fully represented by the BO parameters. Nevertheless, a reasonably good estimate for these two properties can be established solely from a linear combination of electronic structure factors. Furthermore, the TBDO emerges as a significant descriptor that controls the mechanical properties. This data mining approach also demonstrates that a simple correlation can be used to link elastic parameters such as Poisson's ratio or the Pugh ratio to a series of electronic structure indicators. The use of only 50 % of the data as a training set gives credence to the particular machine learning software and the philosophy lying behind it.

4. Further applications of MAX data

Since the generation of the MAX database less than a year ago, additional results that use this data to estimate the lattice thermal conductivity of MAX phases at high temperature and the calculation of universal elastic anisotropy based on a recently developed theory have been obtained. These are prime examples of the utility of large database to easily get new information without lengthy calculations consistent with the spirit of materials informatics. They are briefly described below.

4.1 Lattice thermal conductivity at high temperature

A systematic calculation of the lattice thermal conductivity κ_{ph} and minimum thermal conductivity κ_{min} for the 211, 312, and 413 MAX phases using Slack's equation and the Clarke formula respectively has been carried out [23]. The parameters used in these simplified calculations are extracted from the elastic coefficients C_{ij}, bulk mechanical properties, and equilibrium volume of all stable MAX phase compounds in the database. Essentially, the calculation of κ_{ph}, follows the equation derived by Slack [24],

$$\kappa_{ph} = A\frac{\bar{M}\theta_D^3\delta}{\gamma^2 n^{2/3} T} \quad (1)$$

where $\bar{M}$ is the average atomic weight (in units of kg/mol), δ is the average volume of the mass equivalent to one atom in the primitive cell (in units of m^3), T is the absolute temperature, n is the number of atoms per unit cell, γ the Grüneisen constant derived from Poisson's ratio (υ) and A is a coefficient (in units of W mol/kg/m^2/K^3) that depends on γ as determined by Julian [25]. These parameters can be obtained from the database for the MAX phases.

Figure 9 shows the calculated κ_{ph} for the 211, 312, and 413 phases of MAX carbides and nitrides presented in two separate ways in order to trace the trends associated with variations in the atomic numbers of the "M" and "A" elements. The top panel in **Figure 9** is for "M"-based plots and the lower panel is for "A"-based plots. The x-axis lists the 9 "M" elements and 11 "A" elements for the top and bottom panels respectively. To grasp the variations and overall trends in κ_{ph} more easily,

we employ the following strategy: (1) the data for the carbides (solid circles) and nitrides (open circles) are plotted on the same figure. (2) The horizontal x-axis is arranged in the order of increasing atomic number Z. They are (Sc, Ti, V, Cr, Zr, Nb, Mo, Hf, Ta) for "M" and (Al, Si, P, S, Ga, Ge, As, In, Sn, Tl, Pb) for "A". Further, each column is separated by vertical blocks of differently shaded colors. Each colored area encloses 22 MAX phases with different "A" in the upper panel and 16 MAX phases with different 'M' in the lower panel. (3) The ordering of both 'A' and 'M' in each block is in the order of increasing Z. The two panels contain the same number of data points but they are plotted in different ways to facilitate the observation of trends. (4) The vertical scale (0 to 20 $Wm^{-1}K^{-1}$) for κ_{ph} is kept the same for easy comparison. Despite the overwhelming amount of data, the following trends and observations can be easily discerned with this creative display: (a) The MAX phases with five highest κ_{ph} at 1300K are all nitrides. (b) The Sc-based MAX phases (first panel to the left in the upper panel) in 211 phases are more widely dispersed than those from the 312 and 413 phases. The κ_{ph} for carbides are much smaller than those of nitrides. For the other M panels, nitrides have a lower κ_{ph} than carbides except in the 211 MAX phases where they are mixed. There is also the obvious trend of reduced κ_{ph} as Z increases. This observation is much more pronounced in the variation of "A" for a given "M" than on the variation of "M" for a given "A". Thus, variation in "A" is the major controlling factor for κ_{ph}. They also show more distinctive separations between carbides and nitrides. The trend of reduced κ_{ph} as the Z value of "M" increases is much less pronounced. This is contrary to the notion that "M" should be more influential than "A" since there are more "M" elements in a given MAX phase. (c) In the panels for different "A", data for carbides and nitrides are rather scattered. Within each panel for a fixed "A", the trends of decreasing κ_{ph} with increasing Z value of "M" is much less pronounced in striking contrast with that data for the variation of "A" for a fixed "M". (d) Data for κ_{ph} are more widely distributed and have larger values in 211 phases. They generally scale inversely with layer index n. The calculated data at 1300 K shown in **Figure 9** are in reasonable agreement with the only available experimental data on eight MAX phases (Ti_2AlC, Nb_4AlC_3, Ta_4AlC_3, Nb_2AlC Nb_2SnC, Ta_2AlC, Cr_2AlC, and Ti_3SiC_2) [12].

We used the same data to estimate the intrinsic minimum thermal conductivity κ_{min} in MAX phases which is the lowest value of thermal conductivity for perfect crystals at high temperature when phonons are completely uncoupled and energy is transferred between neighboring atoms over the Debye temperature [24]. According to the simple theory advanced by Clarke, κ_{min} is given by [26]:

$$\kappa_{min} = k_B v_m \Lambda_{min} = k_B v_m \left(\frac{M}{n\rho N_A} \right)^{-2/3} \qquad (2)$$

Where Λ_{min}, N_A, and ρ are the phonon mean free path, Avogadro's constant, and crystal density respectively. The calculated κ_{min} values are consistent with those using Eq. (1) at T = 2000K.

4.2 Universal elastic anisotropy in MAX phases

Recently, Ranganathan and Ostoja-Starzewski [27] developed a new theory for the universal elastic anisotropy A^U for all types of crystals. This gives a single parameter to quantify the crystal anisotropy similar to the Zener anisotropy index [28] which is applicable only to cubic crystals. A^U is given by:

$$A^U = 5(G^V/G^R) + (K^V/K^R) - 6. \quad (3)$$

Here K and G are the bulk and shear moduli and the superscripts V and R stand for the Voigt and Reuss approximations [29],[30], respectively. The Voigt (Reuss) approximation assumed a uniform strain (stress) distribution throughout the structure. These two assumptions give the upper and lower limits of bulk mechanical properties and the averaged value of these two limits is the Hill approximation [31] which is usually the value used to compare with measured data. A^U must be positive, and is usually much less than 2.0, and seldom goes beyond 4.0 [27]. $A^U = 0$ implies zero anisotropy. The large data base of elastic coefficients for MAX phases is ideally suited to evaluate A^U, test the new theory, and to ascertain its efficacy when applied to a single class of ternary hexagonal compounds, the MAX phases.

We have recently calculated the universal elastic anisotropy of the 665 MAX phases according to Eq. (3) [32]. **Figure 10** shows the scattered plot of A^U vs the total bond order density (TBOD) which we advocate as the single most important metric for the electronic part of the properties. Here, A^U is supposed to be a single parameter that describe the anisotropy in mechanical properties for a given crystal. As can be seen, the majority of the MAX phases have a low A^U of less than 0.5 although some phases have A^U greater than 1.0. There is no apparent difference between MAX carbides and MAX nitrides in the A^U distribution, but there is evidence of a bimodal distribution of the data, i.e. there is a broad minimum in the middle range of the TBOD. The implication of this interesting result has yet to be explored.

Figure 11 shows the A^U map for all the MAX phases according to "M" (Y-axis) and "A" (X-axis) elements similar to **Figure 4**. Color in the square cell represents calculated A^U values as indicated in the color bar. Again, a star in the box indicates that the phase has been confirmed. The symbol "+" stands for elastic instability and "×" indicates that the phase is screened out for positive heat of formation. This map clearly shows with a glance that most of the MAX phases have low A^U close to 0.1-0.5 and that all of the confirmed phases have low A^U. Few of the phases with high A^U are easily identified. Once more, we used this innovative map of A^U to easily and clearly show the general trends in universal elastic anisotropy according to this new theory and to identify some isolated MAX phases as outliers.

5. Extension to other materials systems.

5.1 MAX-related systems, MXenes, MAX solid solutions, and similar layered structures.

A newly discovered class of 2D materials, labeled MXenes, presents a unique opportunity for the development of exceptional functional properties with diverse applications [33], [34]. MXenes are anisotropic laminated transition metal compounds derived from predecessor MAX phases. Very

recently, a family of 2D materials was derived from MAX phases by extracting the A element in MAX. These so-called MXenes ($M_{n+1}X_nT_x$), have their surface terminated by T_x (O, OH, or F). Only a few MXenes out of a large number of possibilities have been reported. Some of these MXenes have high electric conductivities with hydrophilic surfaces making them ideal for applications as electrodes in Li-ion batteries or Li-ion capacitors. Demonstration of spontaneous intercalation of cations of different sizes and charges (Li^+, Na^+, K^+, Mg^{2+}, Al^{3+}, $(NH_4)^+$, N_2H_4) between 2D $Ti_3C_2T_x$ surfaces in various salt solutions presents a great opportunity for material tunability. Such a wide range of choices of cation intercalations and the rich chemistry of the functionalized surfaces offer truly unique functional applications beyond the limits of even the most advanced 2D structures. The underlying factors governing the design and syntheses of MXenes however is largely unknown at atomistic-scales. Thus, MXenes are an ideal system to apply the techniques used in materials informatics similar to the ones we used for the MAX phases in creating a database for $M_{n+1}C_n$, $M_{n+1}N_n$, and $M_{n+1}AT_x$.

Another area is to consider extending MAX phases to their solid solutions. This offers a much larger variation in composition range and in the fine tuning of the desired properties. MAX solid solutions can be formed by partial substitutions in "M", "A" elements or between C and N. There have not been many accurate calculations on the MAX solid solutions because such calculations require significant computational resources. Solid solutions are no longer crystalline phases with well-defined long range order. They are essentially a class of disordered solids with random site substitutions. A large number of supercells must be used to properly describe the structure and property variations with composition x. Thus MAX solid solutions offer another great opportunity to apply the methods of materials informatics for extensive studies. The database for MAX phases and their various applications in data mining schemes demonstrated above can facilitate the effort to investigate MAX solid solutions. We have recently carried out a detailed investigation on one of the most important MAX solid solution phases, $Ti_2Al(C_xN_{1-x})$ [35]. For this solid solution, the mechanical properties vary continuously with x between Ti_2AlN and Ti_2AlC with no evidence of improved mechanical parameters beyond the end members. They do have subtle variations for $x > 0.5$ which are supported by some existing experimental observations. This does not rule out the possibility of strengthening MAX phases in other solid solutions via substitutions in "M" or "A" elements.

In addition to MAX solid solutions, another route to significantly enlarge the database of MAX or MAX-like compounds is to consider the quaternary alloys by adding another metal element to create a new crystal structure with different crystal symmetry. A recent example of achieving this goal is the theoretical suggestion of a new compound $(Cr_2Hf)_2Al_3C_3$ [36]. The crystal structure and elastic properties of this MAX-like compound are studied using similar computational methods as in the MAX phases. Unlike MAX phases which have a hexagonal symmetry (space group: $P6_3/mmc$, #194), $(Cr_2Hf)_2Al_3C_3$ crystallizes in the monoclinic structure with a space group of $P2_1/m$ (#11) with lattice parameters $a = 5.1739$ Å, $b = 5.1974$ Å, $c = 12.8019$ Å; $\alpha = \beta = 90°$, $\gamma = 119.8509°$. The calculated total energy per unit cell for this crystal is found to be energetically more favorable than potential competing phases. The calculated total energy per formula unit of −102.11 eV is significantly lower than those of the allotropic segregation (−100.05 eV) and solid solution phases (−100.13 eV). Calculations using a stress versus strain approach and the VRH approximation for polycrystals show that $(Cr_2Hf)_2Al_3C_3$ has outstanding elastic moduli, better than

Cr_2AlC or Hf_2AlC. Obviously, this approach can be used to explore many more new phases with some exotic properties. It is
probably premature to apply techniques of materials informatics to study quaternary MAX-like compounds at this stage unless new creative algorithms can be designed.

5.2 CSH-cement crystals

Cement materials represent another system that is highly amenable for materials informatics. They are very complicated in both composition and structure but have well defined industrial standards for desirable attributes in properties. Most of all, they are of great importance and relevance to the construction industry, the environment, and the world economy. Calcium silicate hydrate (CSH) is the main binding phase of Portland cement, the single most important structural material in use worldwide. Due to the complex structure and chemistry of CSH, accurate computational studies at the atomic level are almost non-existent. Recently, we studied the electronic structure and bonding of a large subset of the known CSH minerals [37]. **Table III** lists the 20 CS and CSH crystal phases with well-documented atomic positions used in this study. They are divided into four groups according to the Strunz scheme [38]: ***a***, Clinker and hydroxide phase; ***b***, nesosubsilicates; ***c***, sorosilicates; and ***d***, ionosilicates. Each group in **Table III** is arranged in ascending order of calcium to silicon (C/S) ratio. The clinker phases (a.1 and a.2 with no H) and the Portlandite (a.3 with no Si) are placed in **group *a***. Portlandite is included in this group because it forms the basis for hydration of cement.

Our results reveal a wide range of contributions from each type of bonding, especially the hydrogen bonding. We find that the total bond order density (TBOD) is again an ideal overall metric for assessing crystal cohesion of these complex materials and should replace the conventionally used Ca/Si ratio. A rarely known orthorhombic phase, Suolunite, is found to have higher cohesion (TBOD) in comparison to Jennite and Tobermorite, which are considered to be the backbone of hydrated Portland cement [37, 39, 40].

Obviously the crystalline CSH phases listed in **Table III** can be greatly expanded to include additional elements such as Al in the Ca-Si-Al-hydrates. A large database of cement crystals similar to the MAX phases can be built for materials informatics to design new construction materials which are more economical, environmentally friendly, and durable. This is another example of using the TBOD as a proper descriptor for materials design.

Table III. List of 20 CS and CSH crystals divided into four groups based upon Strunz classification as discussed in our previous study [37]

	Mineral Name	Sym/space group	Chemical formula	Ca/Si	ρ(g/cc)	TBOD
(a). Clinker/Hydroxide						
a.1	Belite	O: *P 1 21/n 1*	$2(CaO)\ SiO_2$	2.00	3.316	0.0226
a.2	Alite	M:P-1	$3(CaO)\ SiO_2$	3.00	3.084	0.0197
a.3	Portlandite	M: *P -3 m 1*	$Ca(OH)_2$	N/A	2.668	0.0177
(b). Nesosubsilicates						
b.1	Afwillite	M:P1	$Ca_3(SiO_3OH)_2{\cdot}2H_2O$	1.50	2.590	0.0243
b.2	α-C2SH	O: *P 2_1/b 2_1/c 2_1/a*	$Ca_2(HSiO_4)(OH)$	2.00	2.693	0.0216
b.3	Dellaite	Tc:P-1	$Ca_6(Si_2O_7)(SiO_4)(OH)_2$	2.00	2.929	0.0210
b.4	Ca Chondrodite	M: *P 1 1 2_1/b*	$Ca_5[SiO_4]_2(OH)_2$	2.50	2.828	0.0194
(c). Sorosilicates						
c.1	Rosenhahnite	Tc:P-1	$Ca_3Si_3O_8(OH)_2$	1.00	2.874	0.0241
c.2	Suolunite	O: *F d 2 d*	$Ca_2[Si_2O_5(OH)_2]H_2O$	1.00	2.649	**0.0255**
c.3	Kilchoanite	O: *I 2 c m*	$Ca_6(SiO_4)(Si_3O_{10})$	1.50	2.937	0.0209
c.4	Killalaite	M: *P 1 2_1/m 1*	$Ca_{6.4}(H_{0.6}Si_2O_7)_2(OH)_2$	1.60	2.838	0.0217
c.5	Jaffeite	Tg: *P 3*	$Ca_6[Si_2O_7](OH)_6$	3.00	2.595	0.0192
(d). Inosilicates						
d.1	Nekoite	Tc: P1	$Ca_3Si_6O_{15}{\cdot}7H_2O$	0.50	2.204	0.0240
d.2	T11 Å	M: *B 1 1 m*	$Ca_4Si_6O_{15}(OH)_2{\cdot}5H_2O$	0.67	2.396	0.0248
d.3	T14Å	M: *B 1 1 b*	$Ca_5Si_6O_{16}(OH)_2{\cdot}7H_2O$	0.83	2.187	0.0226
d.4	T 9 Å	Tc: C1	$Ca_5Si_6O_{17}\ 5H_2O$	0.83	2.579	0.0247
d.5	Wollastonite	Tc: P-1	$Ca_3Si_3O_9$	1.00	2.899	0.0224
d.6	Xonotlite	Tc: A-1	$Ca_6Si_6O_{17}(OH)_2$	1.00	2.655	0.0214
d.7	Foshagite	Tc: P-1	$Ca_4(Si_3O_9)(OH)_2$	1.33	2.713	0.0211
d.8	Jennite	Tc:P-1	$Ca_9Si_6O_{18}(OH)_6{\cdot}8H_2O$	1.50	2.310	0.0223

5.3 Possible extension to other materials systems: bulk metallic glasses and high entropy alloys

Another promising system for materials informatics are bulk metallic glasses (BMGs) [41] and the related high entropy alloys (HEAs) [42]. Metallic glasses are a special class of non-crystalline solid that are completely different from crystalline metals due to the lack of long-range order. They have many excellent properties and significant potential as next-generation structural materials. However, there is a lack of fundamental understanding about the structure and dynamics of BMGs at the atomic and electronic level despite many years of intense research. Many of the fundamental issues in BMGs require accurate data that can only be obtained by first-principles calculations. Detailed information about the atomic-scale interactions and their implications on the short-range and medium range orders are still missing. Current research efforts appear to focus mostly on the geometrical analysis of structures to explain the mechanical properties, deformation behavior, glass forming ability, etc. We again advocate for the use of TBOD from high quality electronic structure calculations as a useful theoretical metric to characterize the overall properties of a BMG which can be correlated with glass forming ability and other physical properties. The challenges we face are the requirement for both the accuracy and the size of BMG models and the large number of models that are needed to reach valid conclusions. Most conventional BMGs are either binary (e.g. Zr_xCu_{1-x} and Ni_xNb_{1-x}) or ternary alloys such as $Zr_xCu_yAl_z$. However, there are BMGs with more than 3 or 4 components such as such as $Zr_{41.2}Ti1_{3.8}Cu1_{2.5}Ni_{10.0}Be_{22.5}$ (Vitreloy) [43]. In these multi component BMGs, accurate *ab initio* modeling is *sine qua non* because any classical

molecular dynamic simulation are infeasible due to lack or inadequacy of appropriate potentials. The dependence of BMGs on the specific composition requires a large number of calculations to validate any hypothesis.

High-entropy alloys (HEAs) represent another class of systems which are ideal for using a materials informatics approach. Unlike the traditional alloys based on the principal elements (Fe, Ni, Cu, Ti, Zr, Al *etc*.) as the matrix, HEA is essentially an n-component alloy system with $5 \leq n \leq 13$. The % of major (minor) component Xi (Xs) where we have $5\% \leq Xi \leq 35\%$ and Xs is $\leq 5\%$. High-entropy implies high n. The compositional possibilities for HEAs are almost unlimited. They have attracted a great deal of attention in recent years as replacements for traditional alloys such as Ni_3Al, Ti_3Al which have reached their ultimate limit of materials performance. Many new applications in different industrial and medical areas require alloys with special properties such as high hardness and strength at high temperature, resistance to wear and oxidation, low thermal conductivity, special magnetic properties, and easy formation of nanoparticles. The main effects offered by HEA are thermodynamics (the high entropy effect), the dynamic effect, the lattice distortion effect due to different sizes of the elements, and the effect due to interatomic interactions (the so-called cocktail effect).

A major difference between HEAs and BMGs is that the underlying structure for HEAs is crystalline, mostly in fcc lattice or a mixture of fcc and bcc lattice even though both HEAs and BMGs are disordered alloys. HEAs are more suitable for the systematic application of materials informatics tools because the structural part of the alloy is much simpler to model than in BMGs. On the other hand, the challenge is the enormous number of compositional possibilities which will make the database extremely large.

6. Conclusions

In this Chapter, we have discussed the construction and analysis of a large database for a unique class of materials, MAX phases, and we have articulated a specific approach for using *ab initio* data for materials informatics. What we have learned is that materials informatics is extremely useful but also that it faces a lot of challenges. Our approach will need a large amount of computational resources depending on the systems to be studied, but creative planning and targeted application together with the ways and means the data are presented are very important. A data mining approach can be very effective for accelerating the database generation as exemplified by the MAX phase study. The selective process of establishing internal links amongst the potential descriptors is the key. We have also found that the total bond order density (TBOD) is a very useful descriptor for analyzing a variety of properties and in their interpretations. We also described several other material systems that can employ the similar approach for materials informatics research because they share some common attributes with the MAX phase and they also have well-defined descriptors.

Acknowledgements

I acknowledge with thanks the contributions and assistance from Drs. Sitaram Aryal, Yuxiang Mo and Liaoyuan Wang; Professors Michel W. Barsoum, Ridwan Sakidja, and Paul Rulis; Mr. Chamila C. Dharmawardhana, and Mr. Chandra Dhakal.

This work was supported by the National Energy Technology Laboratory (NETL) of the U.S. Department of Energy (DOE) under Grant No. DE-FE0005865. This research used the resources of the National Energy Research Scientific Computing Center (NERSC) supported by the Office of Basic Science of DOE under Contract No. DE-AC03-76SF00098.

References:

1. Vapnik, V., *The nature of statistical learning theory*. 2000: Springer Science & Business Media.
2. Rajan, K., *Materials informatics.* Materials Today, 2005. **8**(10): p. 38-45.
3. Service, R.F., *Materials Scientists Look to a Data-Intensive Future.* science, 2012. **335**(6075): p. 1434-1435.
4. Jiang, P. and X.S. Liu, *Big data mining yields novel insights on cancer.* Nat Genet, 2015. **47**(2): p. 103-104.
5. Balachandran, P.V., S.R. Broderick, and K. Rajan, *Identifying the 'inorganic gene' for high-temperature piezoelectric perovskites through statistical learning*. Vol. 467. 2011. 2271-2290.
6. Nishijima, M., et al., *Accelerated discovery of cathode materials with prolonged cycle life for lithium-ion battery.* Nat Commun, 2014. **5**.
7. Carrete, J., et al., *Finding unprecedentedly low-thermal-conductivity half-Heusler semiconductors via high-throughput materials modeling.* Physical Review X, 2014. **4**(1): p. 011019.
8. Saad, Y., et al., *Data mining for materials: Computational experiments with AB compounds.* Physical Review B, 2012. **85**(10): p. 104104.
9. Bosse, A.W. and E.K. Lin, *Polymer physics and the materials genome initiative.* Journal of Polymer Science Part B: Polymer Physics, 2015. **53**(2): p. 89-89.
10. Broderick, S., et al., *An informatics based analysis of the impact of isotope substitution on phonon modes in graphene.* Applied Physics Letters, 2014. **104**(24): p. 243110.
11. Aryal, S., et al., *A genomic approach to the stability, elastic, and electronic properties of the MAX phases.* physica status solidi (b), 2014. **251**(8): p. 1480-1497.
12. Barsoum, M.W., *MAX Phases: Properties of Machinable Ternary Carbides and Nitrides*. 2013: John Wiley & Sons.
13. Pugh, S.F., *XCII. Relations between the elastic moduli and the plastic properties of polycrystalline pure metals.* The London, Edinburgh, and Dublin Philosophical Magazine and Journal of Science, 1954. **45**(367): p. 823-843.
14. Mo, Y., P. Rulis, and W.Y. Ching, *Electronic structure and optical conductivities of 20 MAX-phase compounds.* Physical Review B, 2012. **86**(16): p. 165122.
15. Wang, L., P. Rulis, and W.Y. Ching, *Calculation of core-level excitation in some MAX-phase compounds.* J. Appl. Phys., 2013. **114**(2): p. -.
16. Hafner, J., J. Furthmüller, and G. Kresse. *Vienna Ab-initio Simulation Package (VASP)*. 1993; Available from: http://www.vasp.at/.
17. Born, M. and K. Huang, *Dynamical Theory of Crystal Lattices* 1956: Clarendon Press.
18. Ching, W.Y. and P. Rulis, *Electronic Structure Methods for Complex Materials: The orthogonalized linear combination of atomic orbitals*. 2012: Oxford University Press. 360.
19. Ahuja, R., et al., *Structural, elastic, and high-pressure properties of cubic TiC, TiN, and TiO.* Physical Review B, 1996. **53**(6): p. 3072-3079.
20. Nagel, S.R. and J. Tauc, *Nearly-Free-Electron Approach to the Theory of Metallic Glass Alloys.* Physical Review Letters, 1975. **35**(6): p. 380-383.

21. Barsoum, M.W., *MAX Phases: Properties of Machinable Ternary Carbides and Nitrideds*. 2013: Wiley-VCH.
22. Hall, M., et al., *The WEKA data mining software: an update.* ACM SIGKDD explorations newsletter, 2009. **11**(1): p. 10-18.
23. Dhakal, C., et al., *Calculation of Lattice Thermal Conductivity of MAX Phases.* Journal of the European Ceramic Society, 2015. **(Submitted)**.
24. Morelli, D.T. and G.A. Slack, *High lattice thermal conductivity solids*, in *High Thermal Conductivity Materials*. 2006, Springer. p. 37-68.
25. Julian, C.L., *Theory of heat conduction in rare-gas crystals.* Physical Review, 1965. **137**(1A): p. A128.
26. Clarke, D.R., *Materials selection guidelines for low thermal conductivity thermal barrier coatings.* Surface and Coatings Technology, 2003. **163**: p. 67-74.
27. Ranganathan, S.I. and M. Ostoja-Starzewski, *Universal Elastic Anisotropy Index.* Physical Review Letters, 2008. **101**(5): p. 055504.
28. Zener, C., *Elasticity and anelasticity of metals*. 1948: University of Chicago press.
29. Voigt, W., *Lehrbuch Der Kristallphysik (mit Ausschluss Der Kristalloptik)*. 1928: B.G. Teubner.
30. Reuss, A., *Berechnung der Fließgrenze von Mischkristallen auf Grund der Plastizitätsbedingung für Einkristalle.* ZAMM - Journal of Applied Mathematics and Mechanics / Zeitschrift für Angewandte Mathematik und Mechanik, 1929. **9**(1): p. 49-58.
31. Hill, R., *The elastic behaviour of a crystalline aggregate.* Proceedings of the Physical Society. Section A, 1952. **65**(5): p. 349.
32. Dharamawardhana, C.C. and W.Y. Ching, *Universal Elastic Anisotropy in MAX phases.* Journal of the American Ceramic Society, 2015. **(To be published)**.
33. Lukatskaya, M.R., et al., *Cation Intercalation and High Volumetric Capacitance of Two-Dimensional Titanium Carbide.* science, 2013. **341**(6153): p. 1502-1505.
34. Naguib, M., et al., *25th Anniversary Article: MXenes: A New Family of Two-Dimensional Materials.* Advanced Materials, 2014. **26**(7): p. 992-1005.
35. Aryal, S., et al., *Elastic and Electronic Properties of $Ti_2Al(C_{1-x}N_x)$ Solid Solutions.* Journal of the European Ceramic Society, 2015. **(Submitted)**.
36. Mo, Y., et al., *Crystal Structure and Elastic Properties of Hypothesized MAX Phase-Like Compound (Cr2Hf)2Al3C3.* Journal of the American Ceramic Society, 2014. **97**(8): p. 2646-2653.
37. Dharmawardhana, C.C., A. Misra, and W.Y. Ching, *Quantum Mechanical Metric for Internal Cohesion in Cement Crystals.* Scientific reports, 2014. **4**: p. 7332.
38. Strunz, H., *Mineralogische Tabellen*. 1982, Leipzig: Akad. Verl.-Ges. Geest u. Portig.
39. Dharmawardhana, C.C., et al., *Role of interatomic bonding in the mechanical anisotropy and interlayer cohesion of CSH crystals.* Cement and Concrete Research, 2013. **52**(0): p. 123-130.
40. Richardson, I.G., *The calcium silicate hydrates.* Cement and Concrete Research, 2008. **38**: p. 137-158.
41. Schroers, J., *Bulk metallic glasses.* Physics Today, 2013. **66**(2): p. 32-37.
42. Yeh, J.W., et al., *Nanostructured High-Entropy Alloys with Multiple Principal Elements: Novel Alloy Design Concepts and Outcomes.* Advanced Engineering Materials, 2004. **6**(5): p. 299-303.
43. Peker, A. and W.L. Johnson, *A highly processable metallic glass: Zr41. 2Ti13. 8Cu12. 5Ni10. 0Be22. 5.* Applied Physics Letters, 1993. **63**(17): p. 2342-2344.

Figure Captions:

Figure 1. Sketch of crystal structures of four MAX phases M_2AX, M_3AX_2, M_4AX_3, M_5AX_4 (i.e. with n = 1,2,3,4).

Figure 2. Shear modulus vs. bulk modulus for 665 screened MAX phases in the database. Solid circles and open circles are for carbides and nitrides respectively. Different color is used for different n in $M_{n+1}AX_n$. Also shown are the locations of other metals and binary MC and MN compounds.

Figure 3. G/K ratio map for 792 MAX phases according to "M" (Y-axis) and "A" (X-axis) elements. Top panel for carbides and lower panel for nitrides. Color in each cell represents the calculated G/K value as indicated in the color bar. A star in the box indicates that this phase has been confirmed. "+" means the phases is eliminated for elastic instability and "×" means the phase is screened out for thermodynamic instability or positive HoF.

Figure 4. Plot of DOS at Fermi level $N(E_F)$ against total number of valence electrons per unit volume for the 665 MAX phases in the database. Solid symbols for carbides and open symbols for nitrides. Note the outlying nature of the data for the M = Sc with X = C MAX phases.

Figure 5. Flow chart of the approach used for data mining in materials informatics for MAX phases.

Figure 6. Comparison of (a) C_{11}, (b) C_{33}, and (c) C_{13} of 211 MAX carbides obtained from *ab initio* calculations (x-axis) and those from the data mining prediction (y-axis).

Figure 7. Top panel: Use of 50% of MAX data for bulk modulus K as training set to predict the other 50% by comparing with *ab initio* data for 665 MAX phases. Lower panel: relative contribution from different electronic structure descriptors.

Figure 8. Same as Figure 7 but for the shear modulus.

Figure 9. Scatter plots of calculated phonon thermal conductivity (κph) at 1300K of MAX phases: (a) 211 in "M" trend; (b) 211 in "A" trend; (c) 312 in "M" trend; (d) 312 in "A" trend; (e) 413 in "M" trend, (f) 413 in "A" trend. The trend for "M" elements (Sc, Ti, V, Cr, Zr, Nb, Mo, Hf and Ta) and "A" elements (Al, Si, P, S, Ga, Ge, As, In, Sn, Tl and Pb) are along the x-axis in upper and lower panels, respectively. Each differently colored subpanel contains 22 and 18 MAX phases for the top and bottom respectively.

Figure 10. Universal elastic anisotropy (A^U) vs. total bond order density (TBOD) for 665 MAX carbides and nitrides in the database. There is evidence of a bimodal distribution with a minimum in A^U corresponding to a TBOD near 0.035.

Figure 11. Universal elastic anisotropy (A^U) maps for 792 MAX phases according to "M" (y-axis) and "A" (x-axis) elements. The description is the same as for Figure 4 for the G/K map.

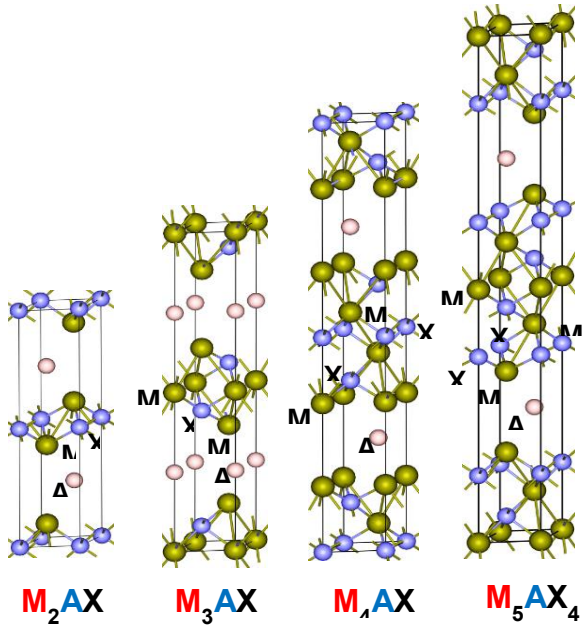

Figure 1. Sketch of crystal structures of four MAX phases M_2AX, M_3AX_2, M_4AX_3, M_5AX_4 (i.e. with n = 1,2,3,4.)

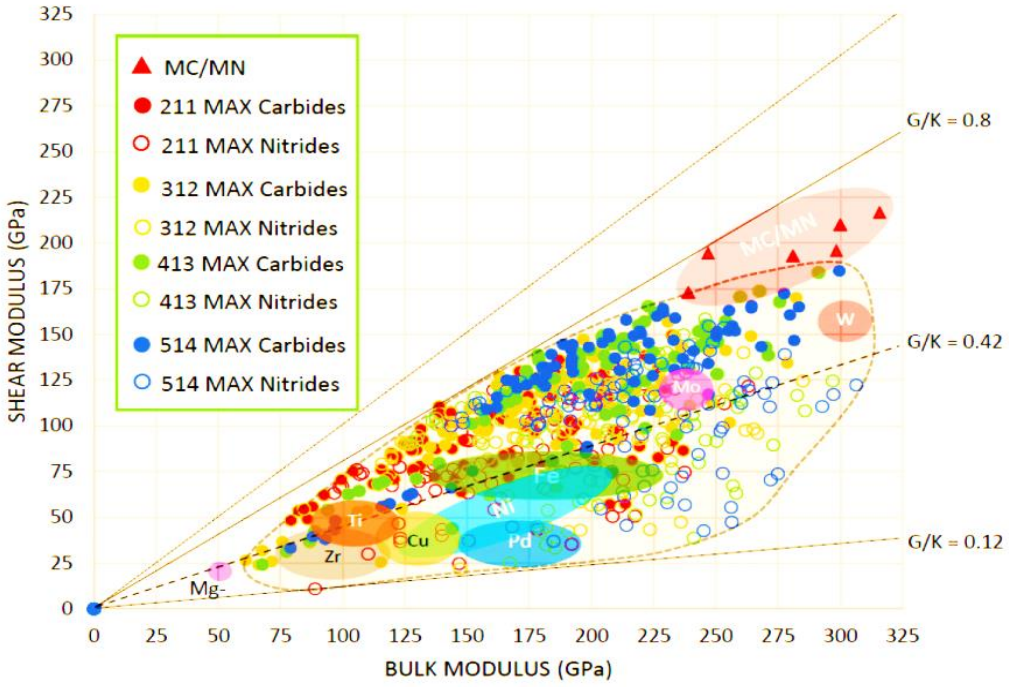

Figure 2. Shear modulus vs. bulk modulus for 665 screened MAX phases in the database. Solid circles and open circles are for carbides and nitrides respectively. Different color is used for different n in $M_{n+1}AX_n$. Also shown are the locations of other metals and binary MC and MN compounds.

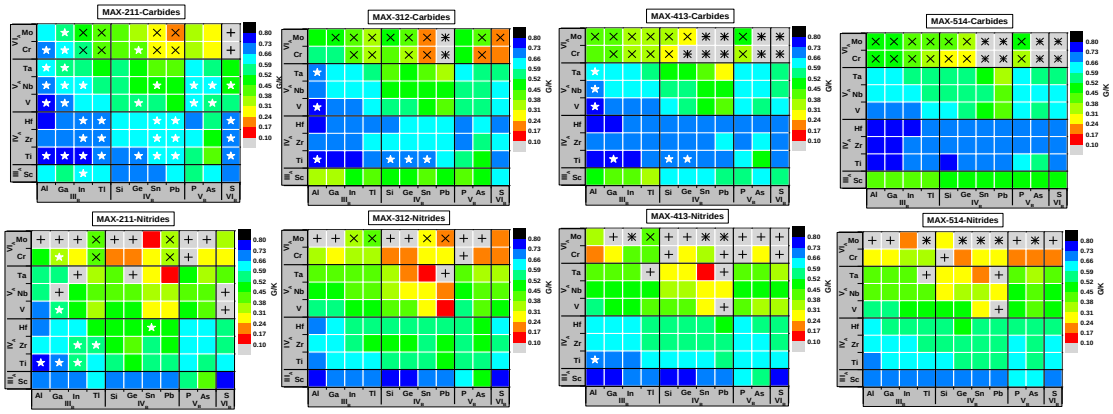

Figure 3. G/K ratio map for 792 MAX phases according to "M" (Y-axis) and "A" (X-axis) elements. Top panel for carbides and lower panel for nitrides. Color in each cell represents the calculated G/K value as indicated in the color bar. A star in the box indicates that this phase has been confirmed. "+" means the phases is eliminated for elastic instability and "×" means the phase is screened out for thermodynamic instability or positive HoF.

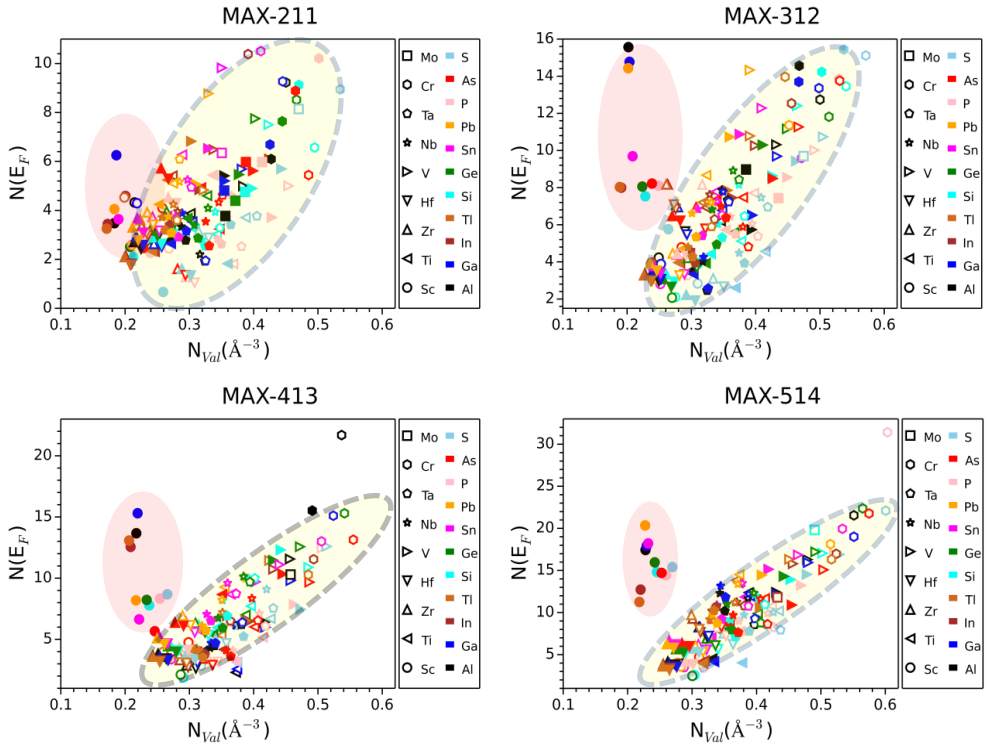

Figure 4. Plot of DOS at Fermi level $N(E_F)$ against total number of valence electrons per unit volume for the 665 MAX phases in the database. Solid symbols for carbides and open symbols for nitrides. Note the outlying nature of the data for the M = Sc with X = C MAX phases.

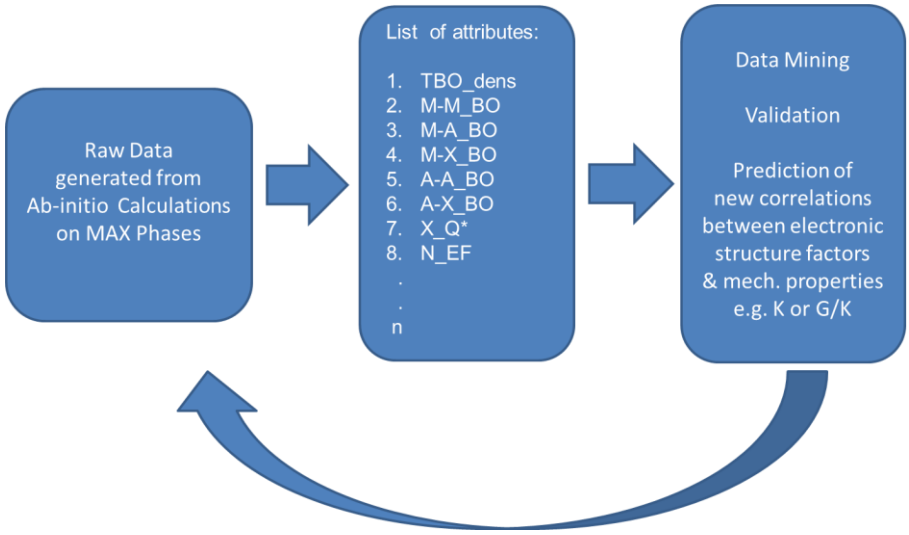

Figure 5. Flow chart of the approach used for data mining in materials informatics for MAX phases.

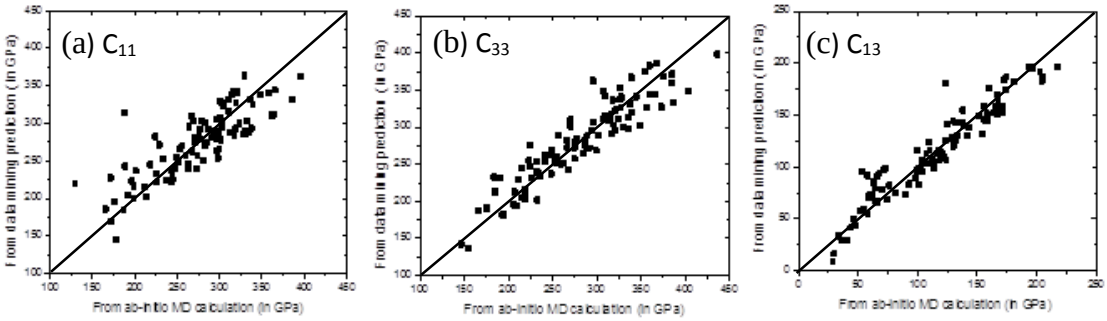

Figure 6. Comparison of (a) C_{11}, (b) C_{33}, and (c) C_{13} of 211 MAX carbides obtained from *ab initio* calculations (x-axis) and those from the data mining prediction (y-axis).

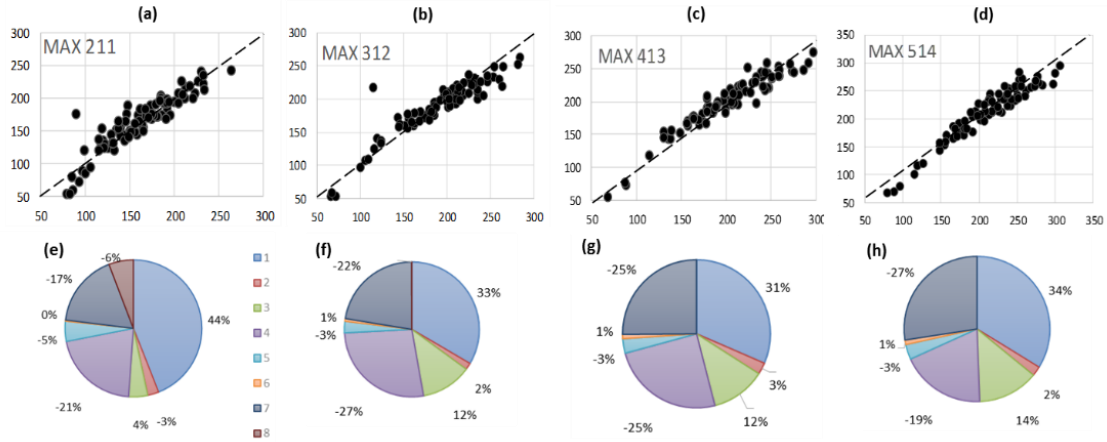

Figure 7 Top panel: Use of 50% of MAX data for bulk modulus K as training set to predict the other 50% by comparing with *ab initio* data for 665 MAX phases. Lower panel: relative contribution from different electronic structure descriptors.

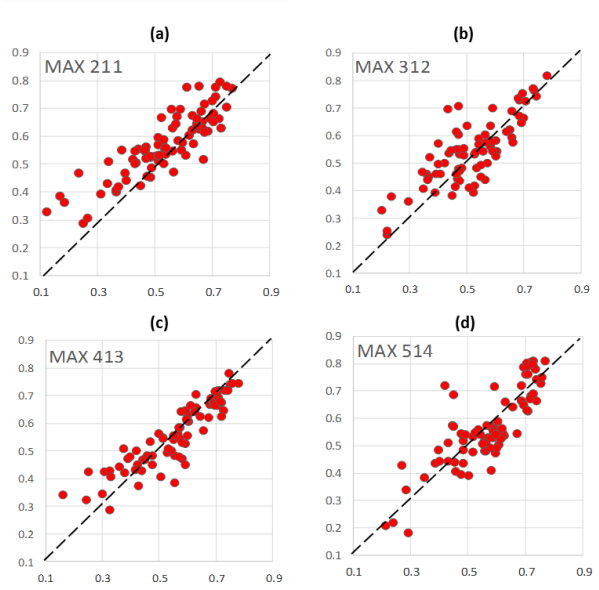

Figure 8. Same as Figure 7 but for the shear modulus.

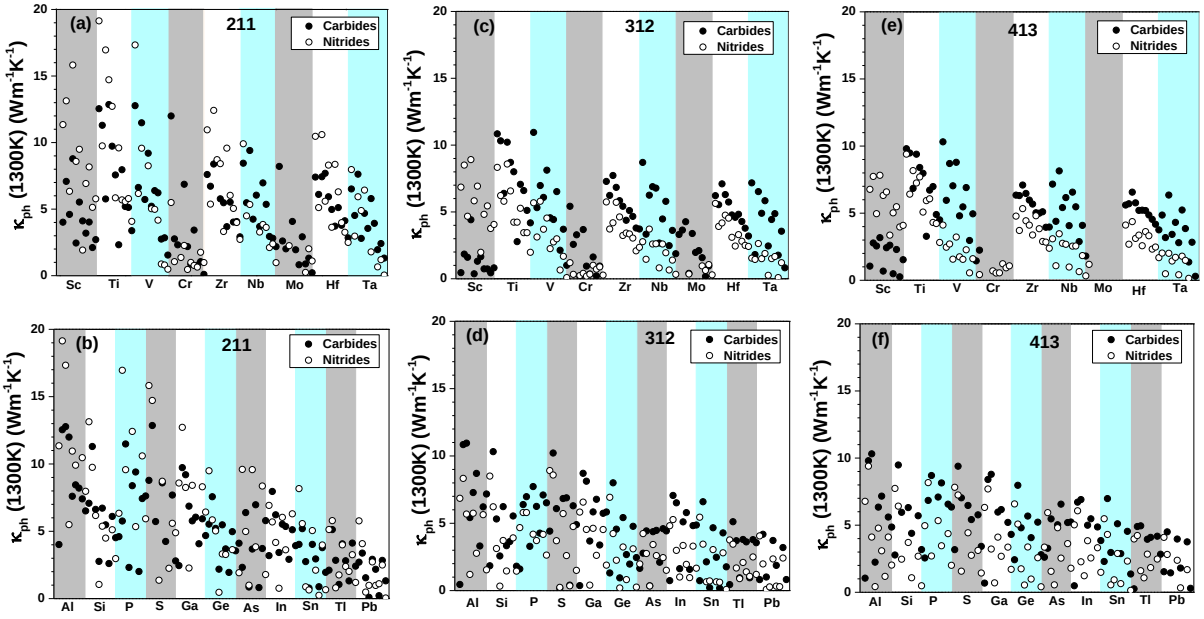

Figure 9. Scatter plots of calculated phonon thermal conductivity (κ_{ph}) at 1300K of MAX phases: (a) 211 in "M" trend; (b) 211 in "A" trend; (c) 312 in "M" trend; (d) 312 in "A" trend; (e) 413 in "M" trend, (f) 413 in "A" trend. The trend for "M" elements (Sc, Ti, V, Cr, Zr, Nb, Mo, Hf and Ta) and "A" elements (Al, Si, P, S, Ga, Ge, As, In, Sn, Tl and Pb) are along the x-axis in upper and lower panels, respectively. Each differently colored subpanel contains 22 and 18 MAX phases for the top and bottom respectively.

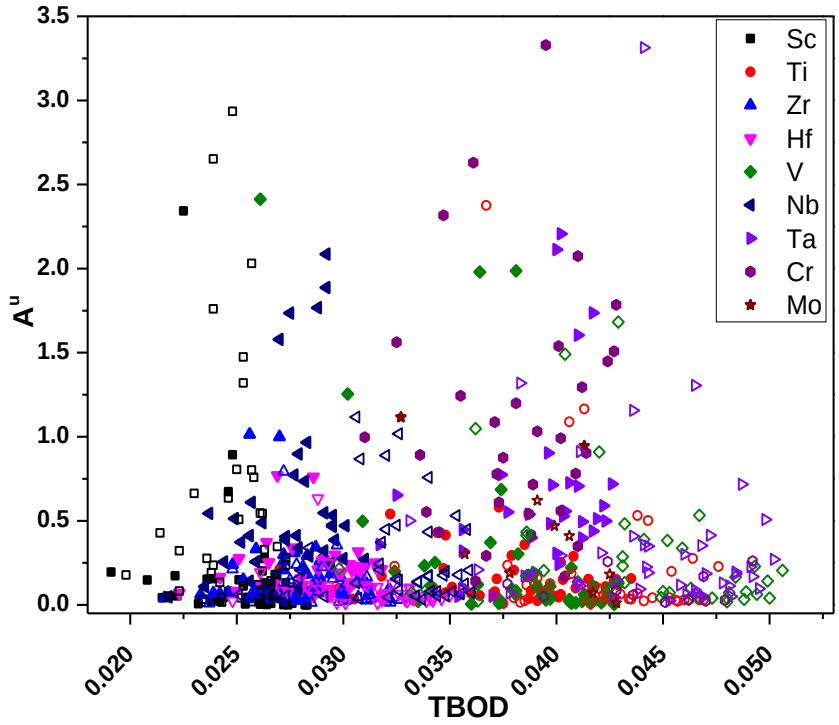

Figure 10. Universal elastic anisotropy (A^U) vs. total bond order density (TBOD) for 665 MAX carbides and nitrides in the database. There is evidence of a bimodal distribution with a minimum in A^U corresponding to a TBOD near 0.035.

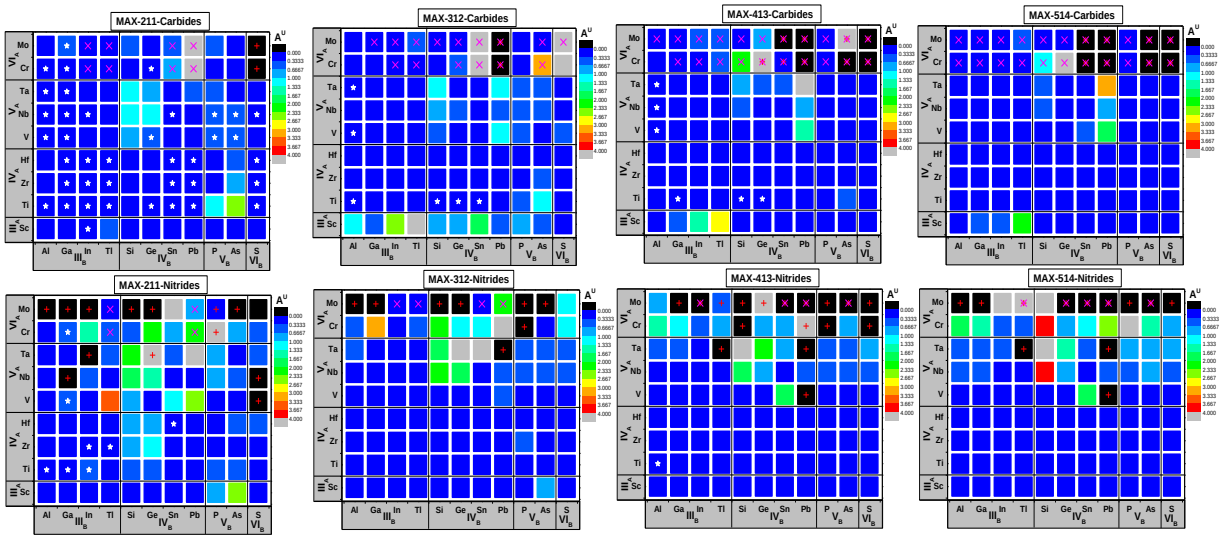

Figure 11. Universal elastic anisotropy (A^U) maps for 792 MAX phases according to "M" (y-axis) and "A" (x-axis) elements. The description is the same as for Figure 4 for the G/K map.